Acoustical Society of America
Acoustics’08 Paris

Geoacoustic inversion using combustive sound source signals

Gopu Potty and James H. Miller
University of Rhode Island, Narragansett, RI

Preston S. Wilson
University of Texas, Austin, TX

James F. Lynch & Arthur Newhall
Woods Hole Oceanographic Institution, Woods Hole, MA

Work supported by Office of Naval Research code 321OA

Outline

- SW-06 Experiment –
  – Combustive Sound Source (CSS) deployment
  – Background geoacoustic data
- CSS data analysis using Dispersion Based STFT (D-STFT)
- Inversion and results
  – Compressional wave speeds
  – Compressional wave attenuation

Potty, Miller, Wilson, Lynch and Newhall, "Geoacoustic inversion using combustive sound sources," JASA-EL (SW06 Special Issue-accepted)

SW 06 – Experimental Area

SW06 Acoustics Moorings

WHOI moored sources/receivers

Sources: MSM, nrl300, nrl500, WHOI224, WHOI400

Receivers: 5 **SHRU**s, Shark

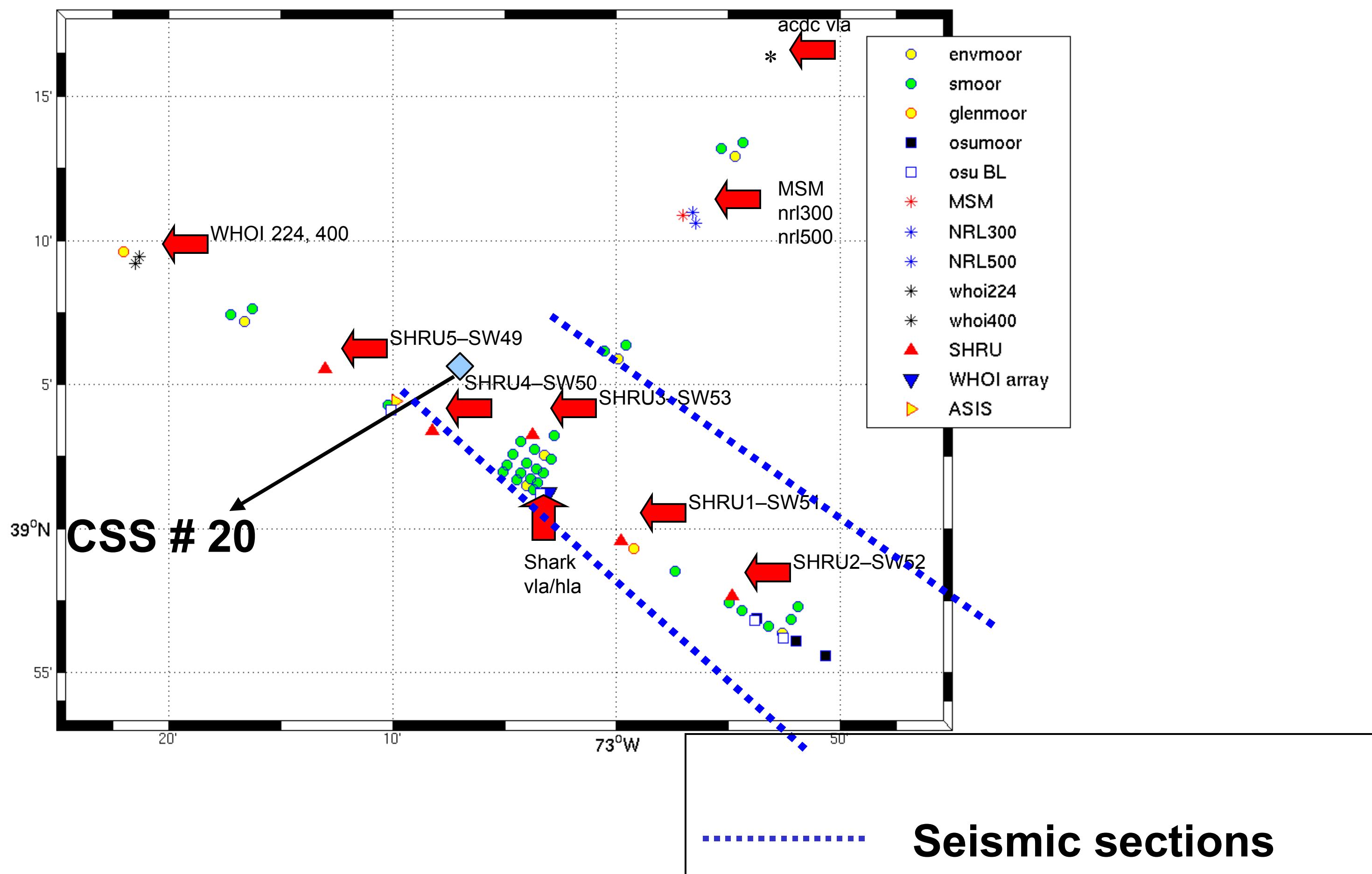

Ocean Sound Speed

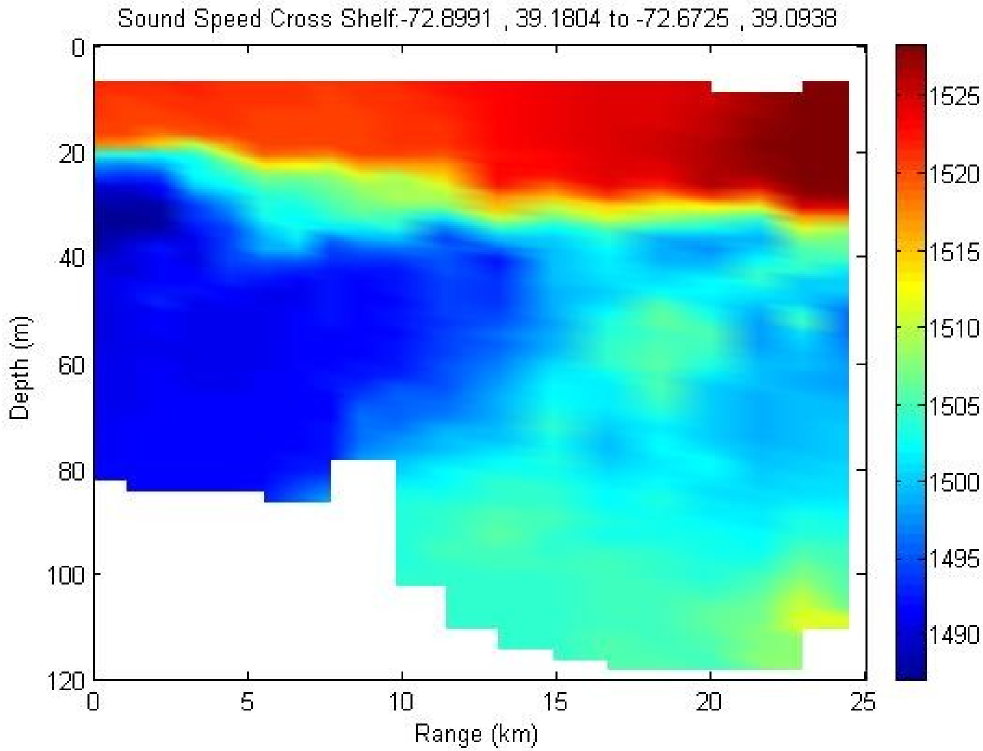

Cross shelf variation of sound speed in the New Jersey shelf measured using a scanfish.

Color scale represents sound speed in m/s.

SHRU being deployed

Bathymetry, Source and Receiver locations

CSS # 20
39^0 5.5174'
-73^0 5.5816

SHRU # 2
38^0 57.6715'
-72^0 54.8139'

Deployed at 107 m

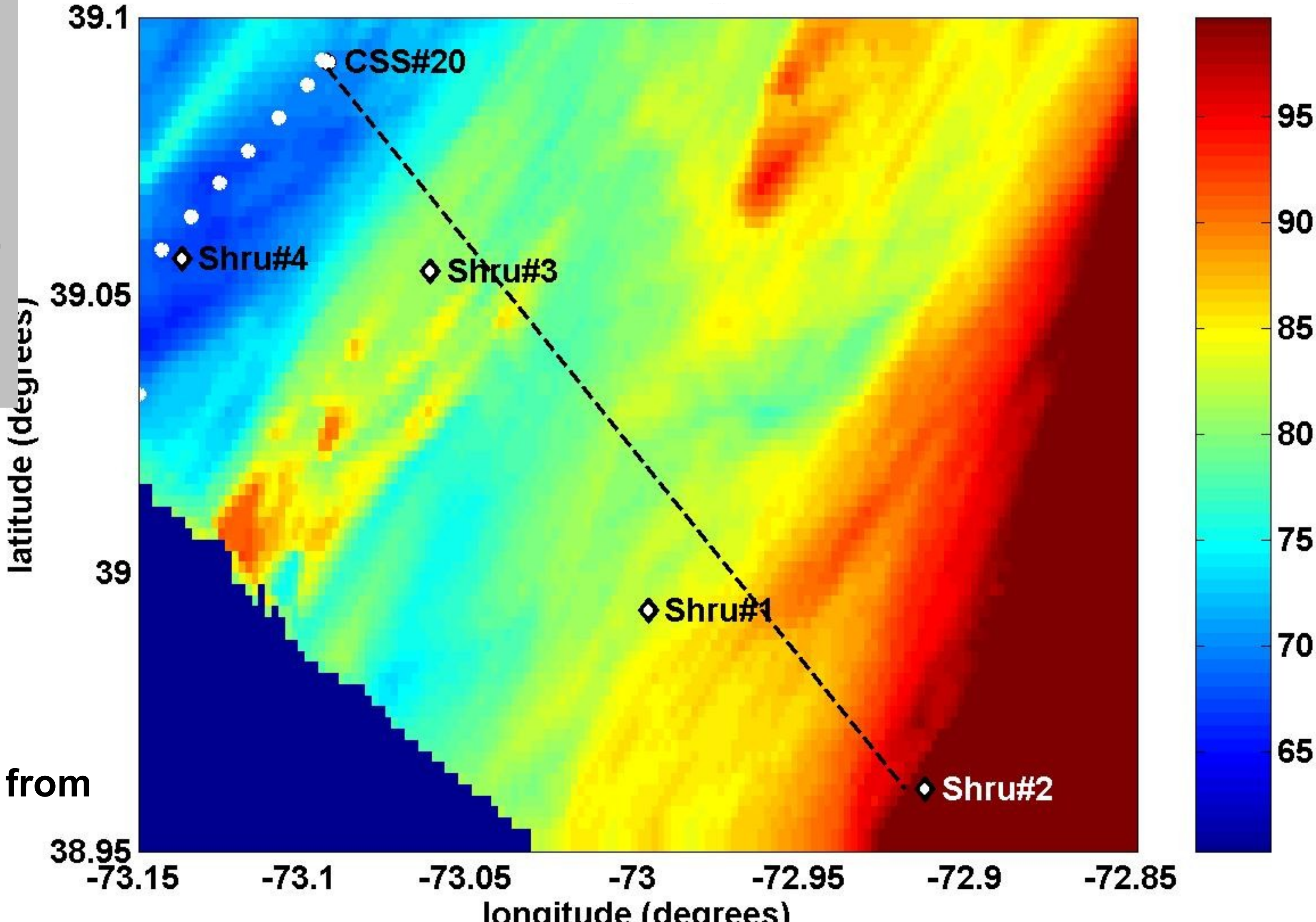

Bathymetry from John Goff

Geo-acoustic data

Range section	Depth (m)	Length (km)
4	100-95	1.44
5	95-90	1.04
6	90-85	3.68
7	85-80	11.27
8	80-75	1.18
9	75-70	2.63

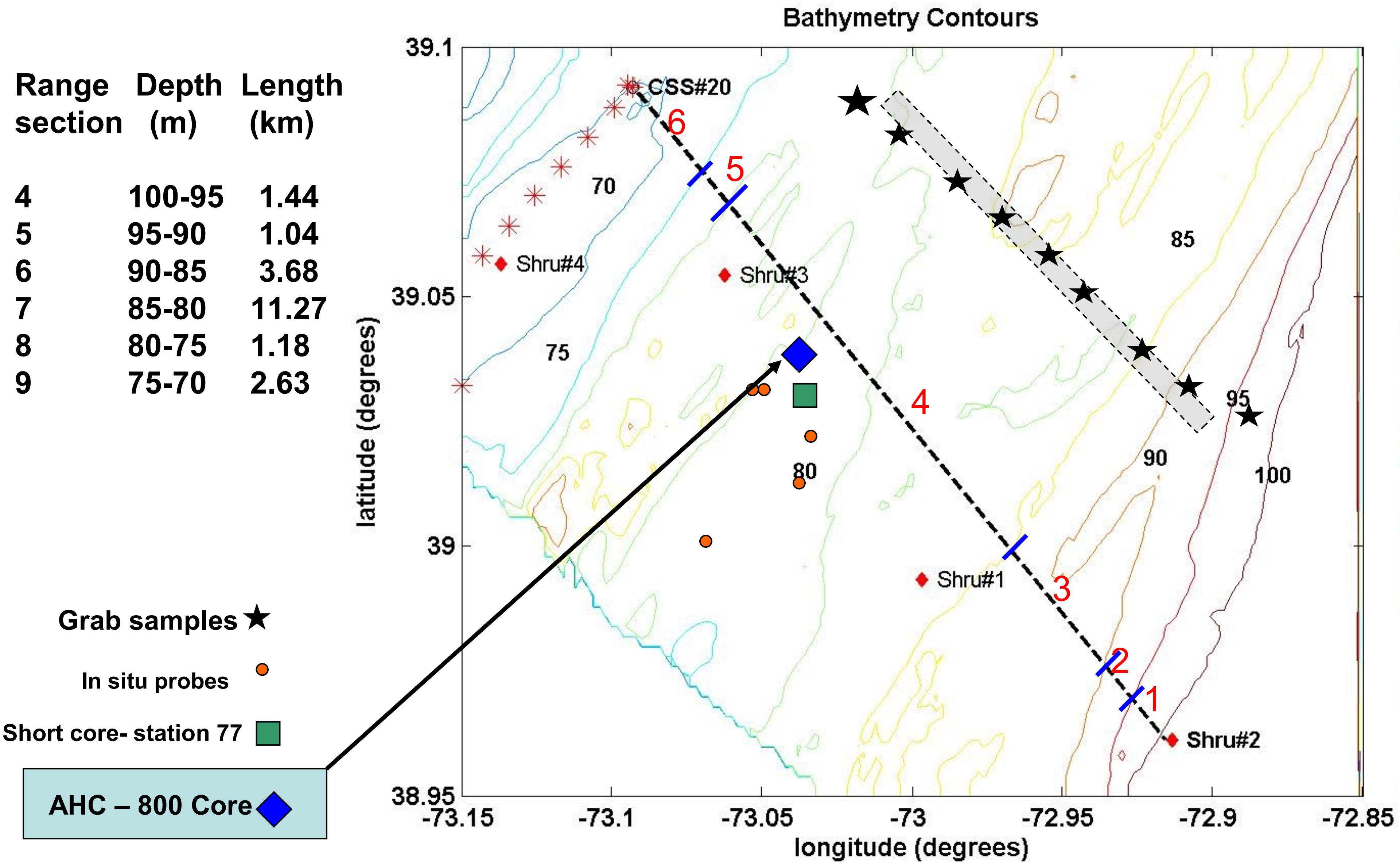

Geoacoustic Model : Jiang et al.

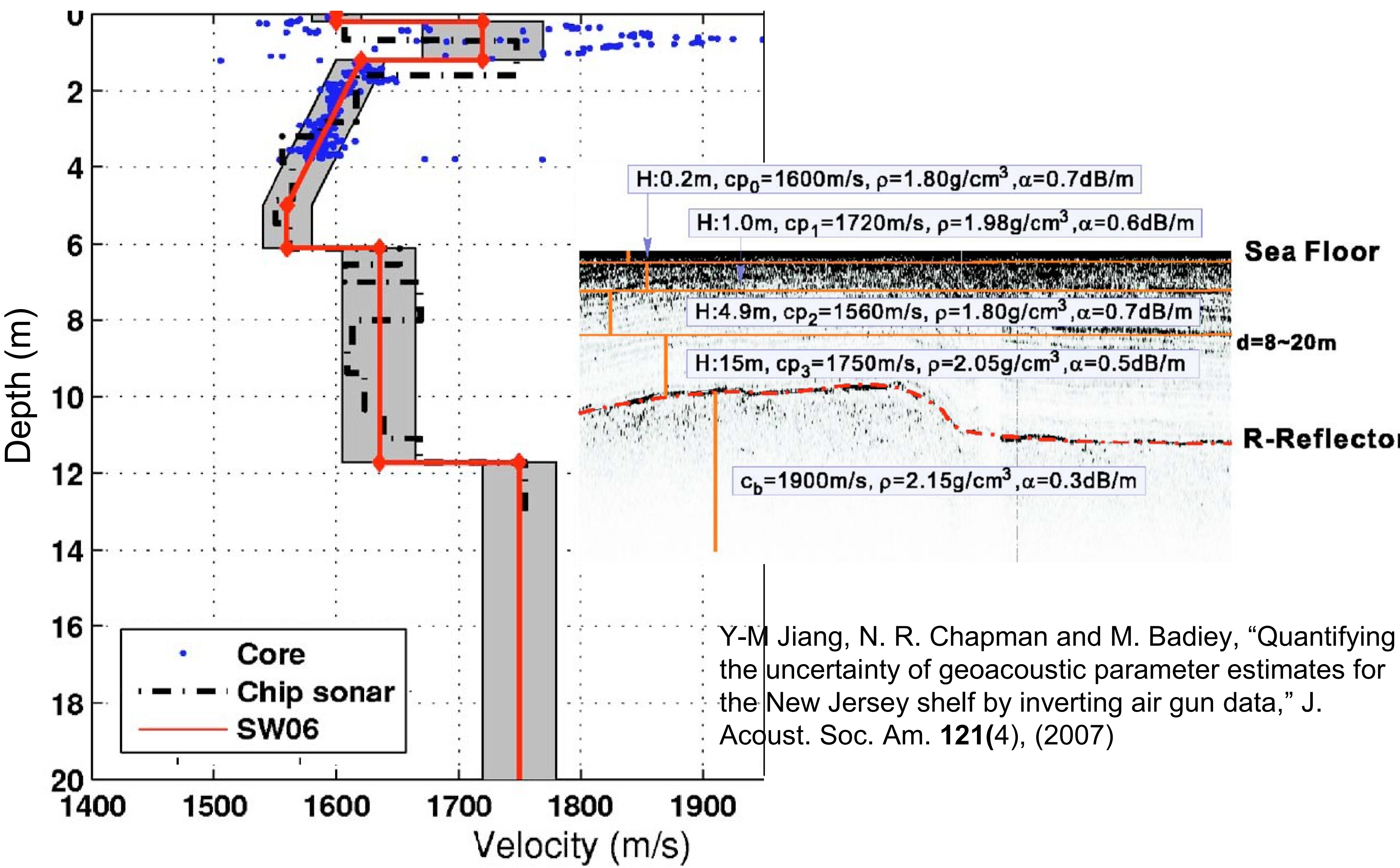

Y-M Jiang, N. R. Chapman and M. Badiey, "Quantifying the uncertainty of geoacoustic parameter estimates for the New Jersey shelf by inverting air gun data," J. Acoust. Soc. Am. **121(**4), (2007)

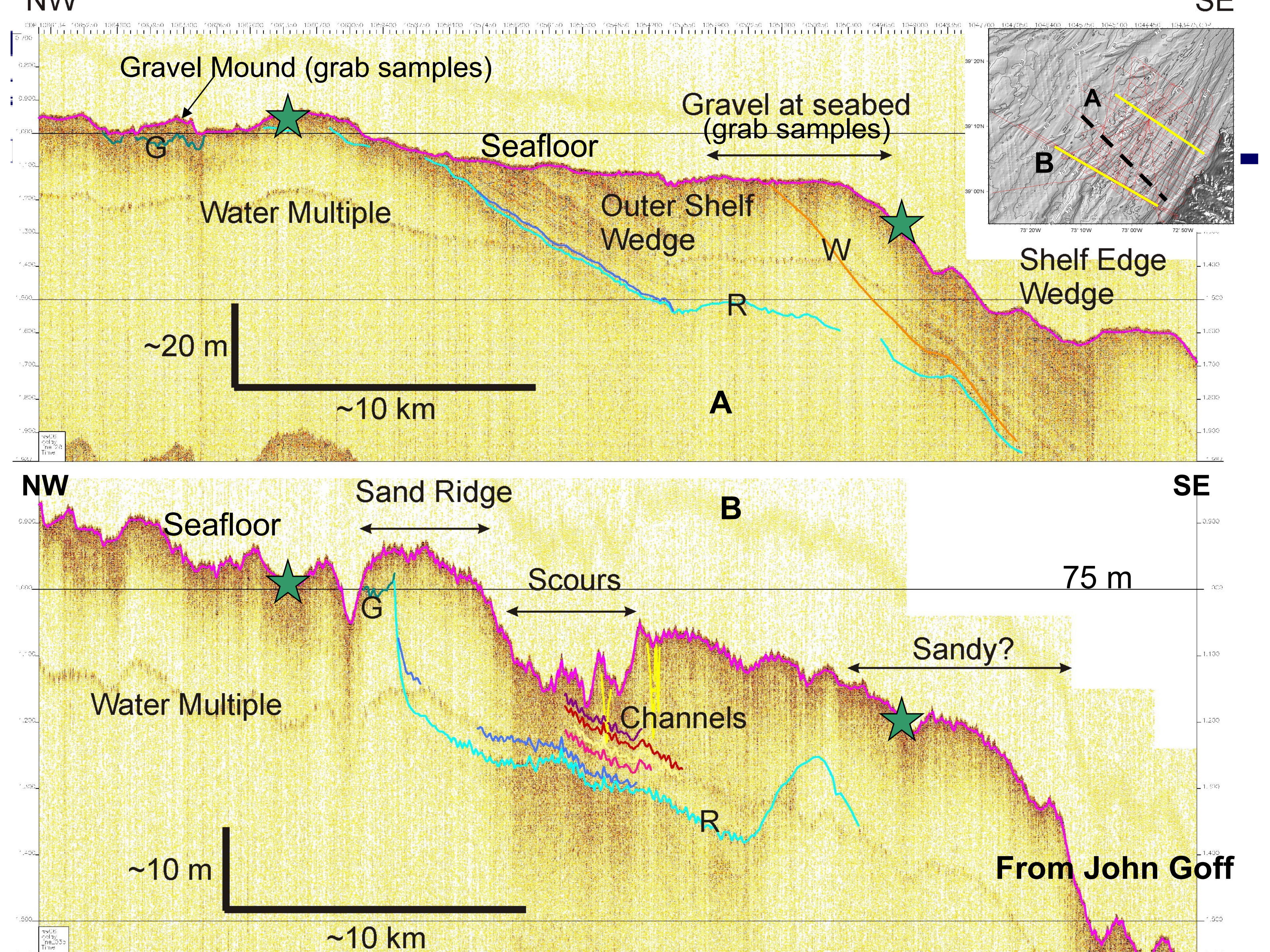
NW
SE
Gravel Mound (grab samples)
G
Seafloor
Gravel at seabed (grab samples)
Water Multiple
Outer Shelf Wedge
W
Shelf Edge Wedge
R
~20 m
~10 km
A
B
NW
SE
Sand Ridge
Seafloor
B
Scours
75 m
G
Sandy?
Water Multiple
Channels
R
~10 m
From John Goff
~10 km

Combustive Sound Source (CSS)

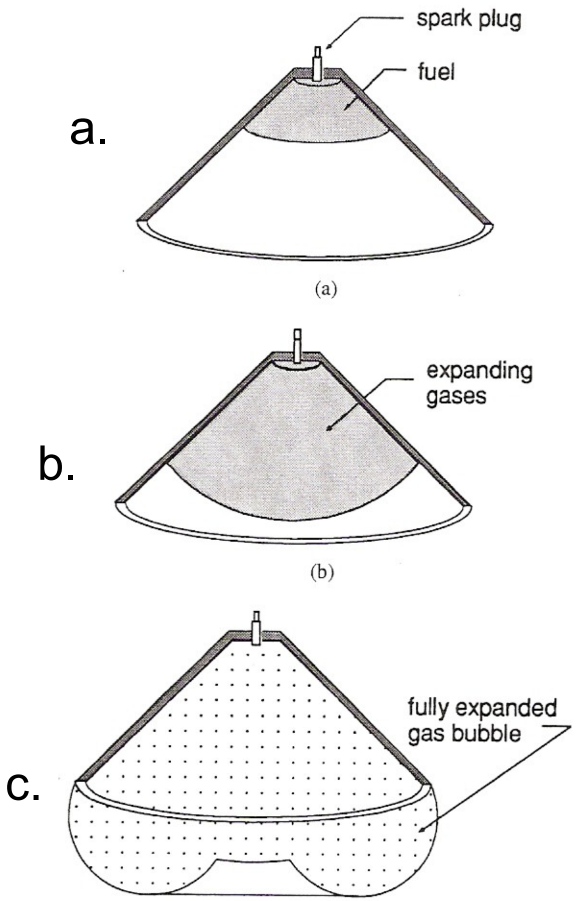

Cross section of CSS combustion Chamber

b. Unburnt gaseous fuel/oxygen mixture

c. Gases expand during combustion

d. Bubble assumes a toroidal shape upon full expansion

From: Wilson, P. S, Ellzey, J. L., and Muir, T. G., "Experimental Investigation of the Combustive Sound Source," IEEE J. Oceanic. Eng., 20(4), 1995.

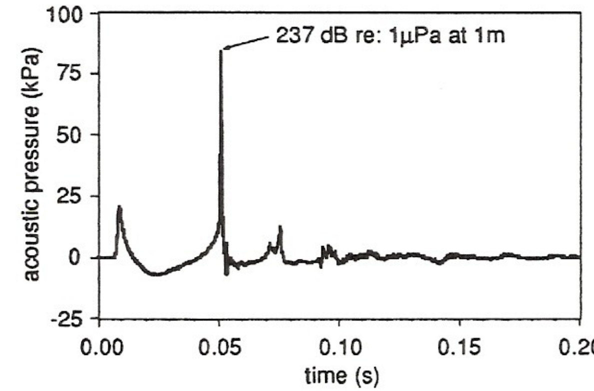

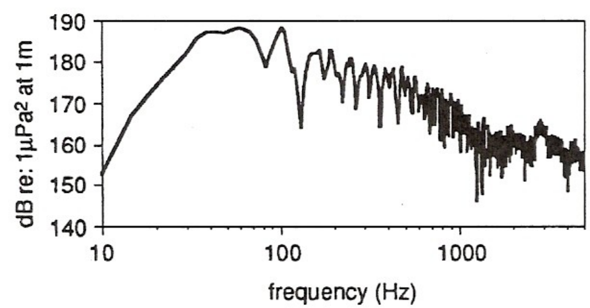

A typical CSS pressure signature (produced by the combustion of 5.0 l stoichiometric hydrogen and oxygen and the power spectrum

The chamber used in SW06 was a cylinder with a hemispherical cap. The bubble motion is not the same for the cylinder and the cone, although the radiated acoustic pulse is similar.

Schematic of CSS Deployment Used in SW06

1) generate gas/load chamber 2) deploy to depth and fire

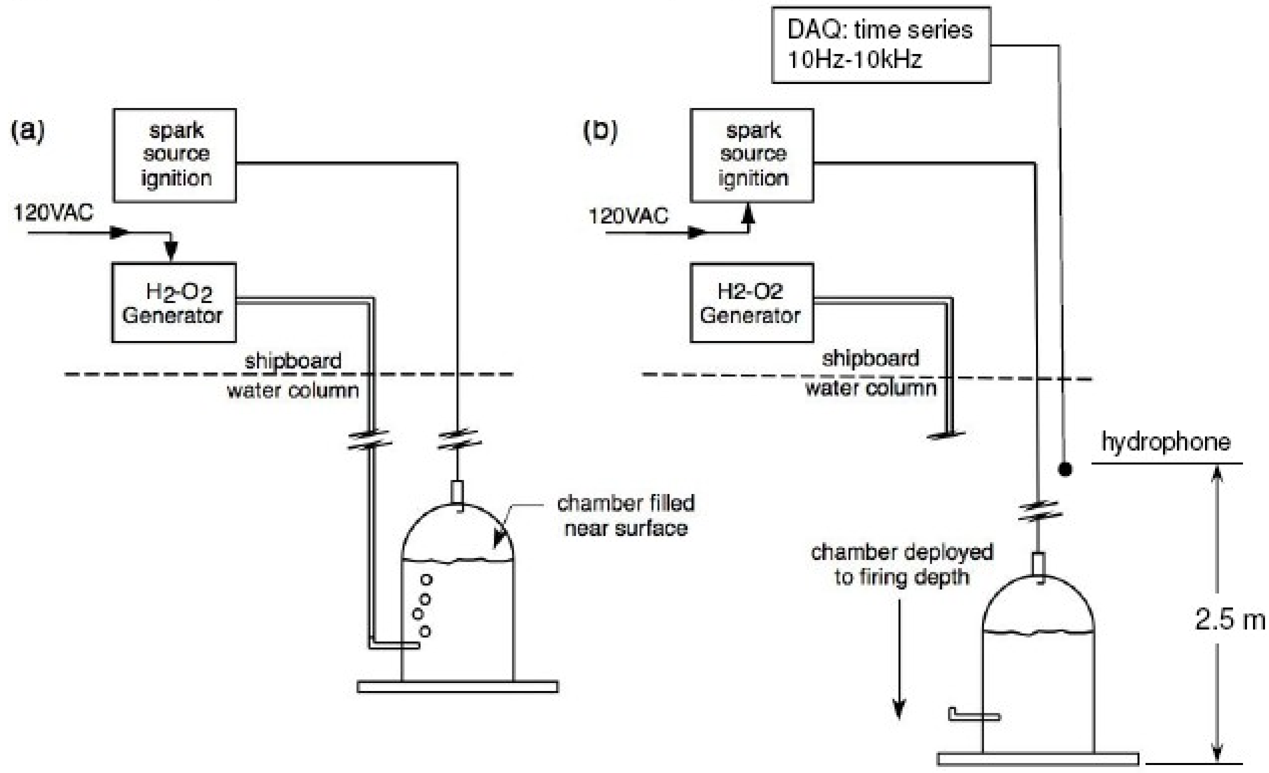

SW06 CSS System

Combustive Sound Source (CSS) during SW-06

- ARL group (Preston Wilson and David Knobles) deployed 31 CSS shots from R/V Knorr
- Depth of CSS ~26 m
- There was a monitoring hydrophone
- Difficult to deploy especially in rough seas

CSS was used as a boot-strap measure to field an impulsive sound source during SW-06. At the time, CSS had been inactive for a decade, and had never been developed beyond the proof-of-concept stage. The device deployed during SW06 was designed for a laboratory engineering study and was not designed to be used at sea. ARL will be working on a more field-able version of CSS.

CSS Signal on a WHOI SHRU

SHRU-1 (Single Hydrophone Receive Unit) – deployed at 85 m; sampled @ 9765 Hz

CSS –Event 2 at Range - 15.2747 km

First two modes strong; higher modes comparatively weak

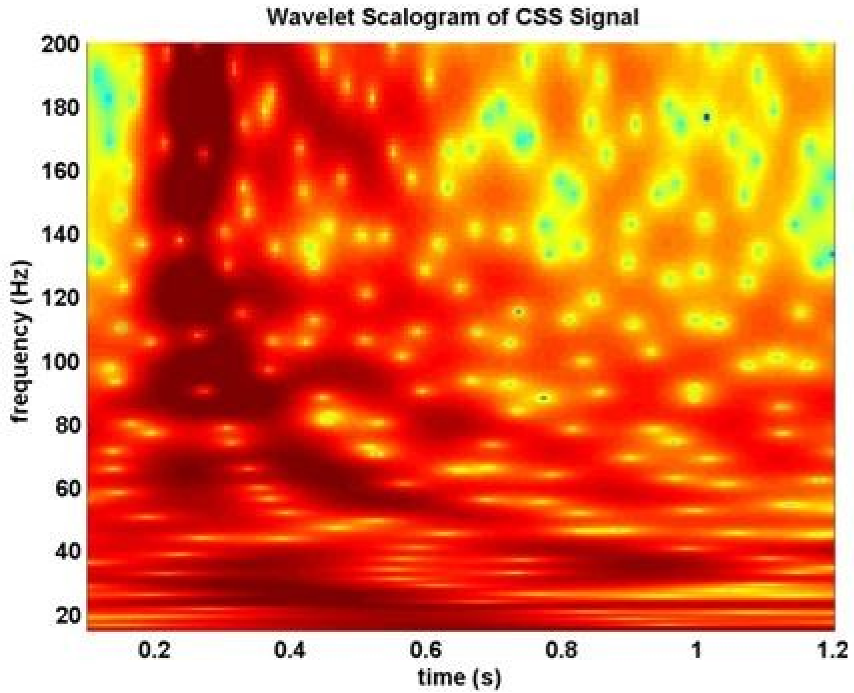

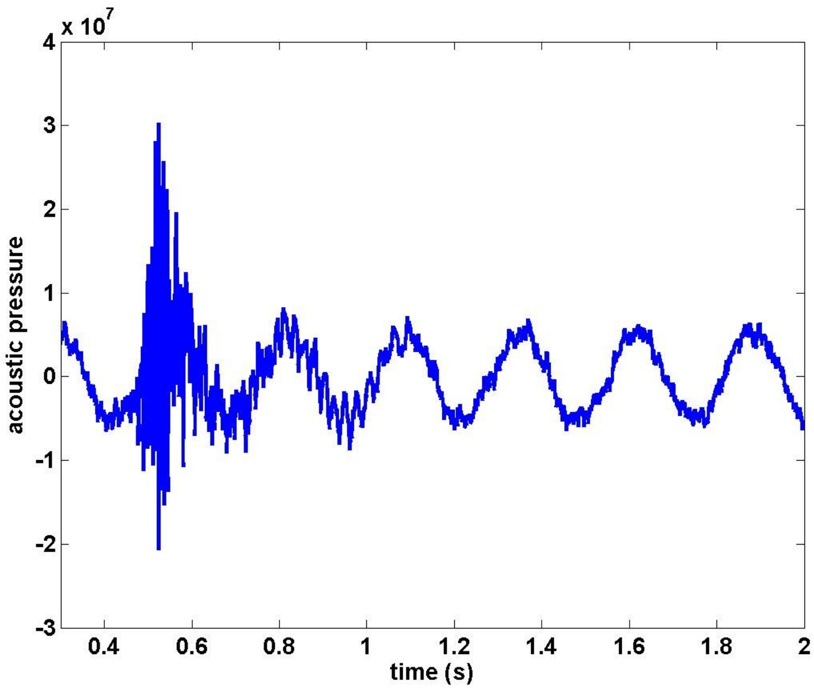

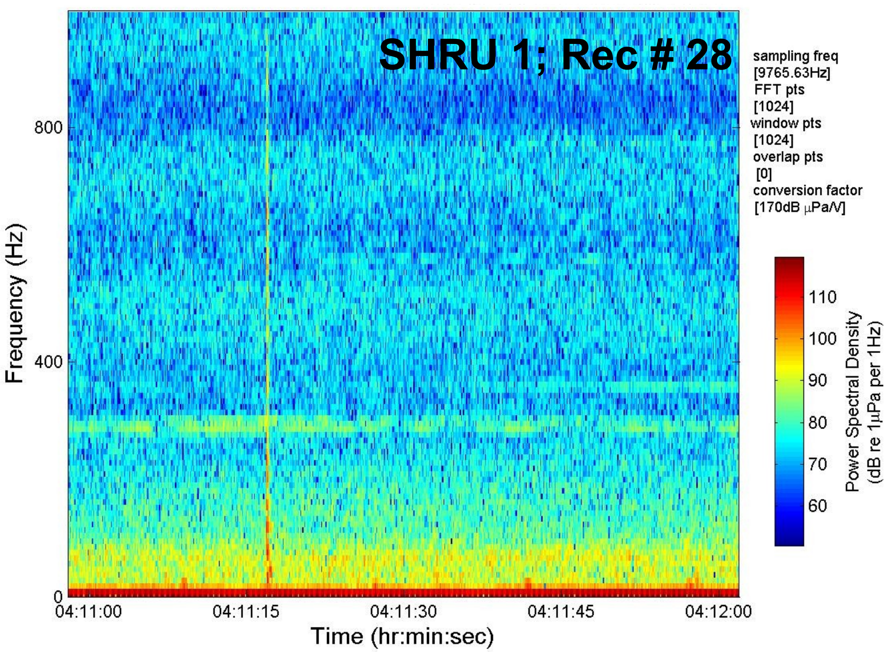

Explosive Sources and CSS

UNIVERSITY OF Rhode Island

Range: 40 km
Water depth ≅ 10
Charge Weight: (
Source depth: 18

Arrival spread 4 s a

PR

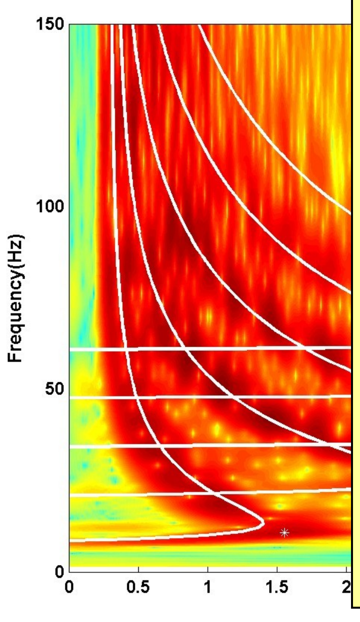

Range: 21.24 km
Water depth ≅ 90 m
Source depth: 26 m

Arrival spread 1 s and 10- 200 Hz.

CSS- SW06

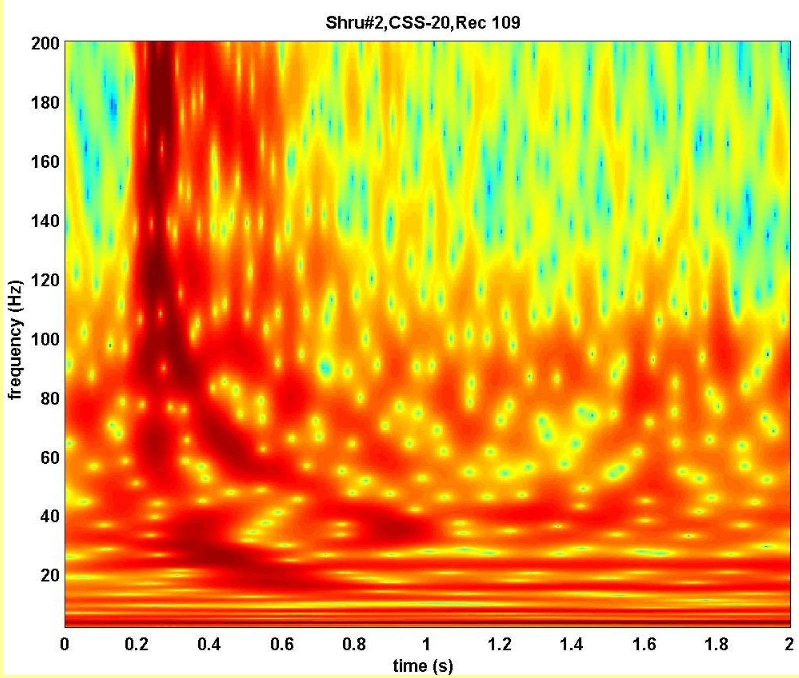

- **CSS is not intended to be a direct replacement for explosives**
- **It is intended to offer a sharp impulse, and have good low-frequency energy, but still more environmentally friendly.**

CS Shot 60

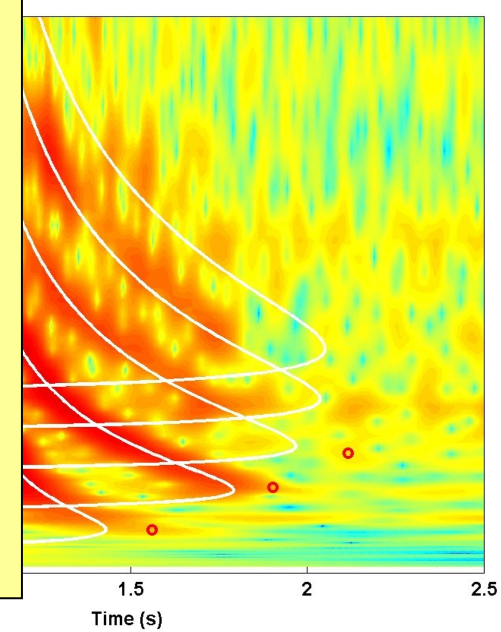

Time- Frequency Analysis Techniques

The short-time Fourier transform (STFT) and the continuous wavelet transform (CWT) are commonly used for the time - frequency analysis of dispersive waves.

The time-frequency resolution achieved by the STFT is independent of the location in the time-frequency plane; CWT allows frequency-adaptive time-frequency tiling

Time-frequency tilings of STFT and CWT do not consider the dispersion effect explicitly.

Hong et al. developed an adaptive time-frequency analysis method, whose time-frequency tiling depends on the dispersion characteristics of the wave signal to be analyzed

---

Jin-Chul Hong, Kyung Ho Sun, and Yoon Young Kim, “Dispersion-based short-time Fourier transform applied to dispersive wave analysis,” J. Acoust. Soc. Am. **117** (5), May 2005

Short time Fourier Transform

$$Sf(u,\xi) = \int_{-\infty}^{\infty} f(t)\bar{g}_{(s,u,\xi)}dt$$

$$= \int_{-\infty}^{\infty} f(t)\frac{1}{\sqrt{s}}g\left(\frac{t-u}{s}\right)e^{-i\xi t}dt$$

$$g_{(s,u,\xi)}(t) = \frac{1}{\sqrt{s}}g\left(\frac{t-u}{s}\right)e^{-i\xi t}$$

Window function g(t) is a Gaussian

$$\mathrm{g(t)} = \pi^{-1/4}e^{-\frac{t^2}{2}}$$

$$\left\{\begin{array}{l}\bar{g}\ \text{denotes the complex conjugate of g} \\ \text{s determines the size of the window}\end{array}\right\}$$

Dispersion based Short time Fourier transforms

$$Df(u,\xi) = \int_{-\infty}^{\infty} f(t)\overline{g}_{(s,u,\xi,d)}(t)dt$$

$$= \int_{-\infty}^{\infty} f(t)\left[\frac{1}{\sqrt{s}}g\left(\frac{t-u}{s}\right)\otimes (id)^{-1/2}e^{-i\left(\frac{t^2}{2d}\right)}\right]e^{-i\xi t}dt$$

$$g_{(s,u,\xi)}(t) = \left[\frac{1}{\sqrt{s}}g\left(\frac{t-u}{s}\right)\otimes (id)^{-1/2}e^{-i\left(\frac{t^2}{2d}\right)}\right]e^{-i\xi t}$$

Window function g(t) is a Gaussian

$$g(t) = \pi^{-1/4}e^{-\frac{t^2}{2}}$$

$$\left\{\begin{array}{l}\overline{g} \text{ denotes the complex conjugate of g} \\ \text{s determines the size of the window}\end{array}\right\}$$

Dispersion based Short time Fourier transforms

d determines the amount of rotation of the time - frequency box in (u,ξ)

$$d = d(u,\xi) = \frac{\Delta u}{\Delta \xi}$$

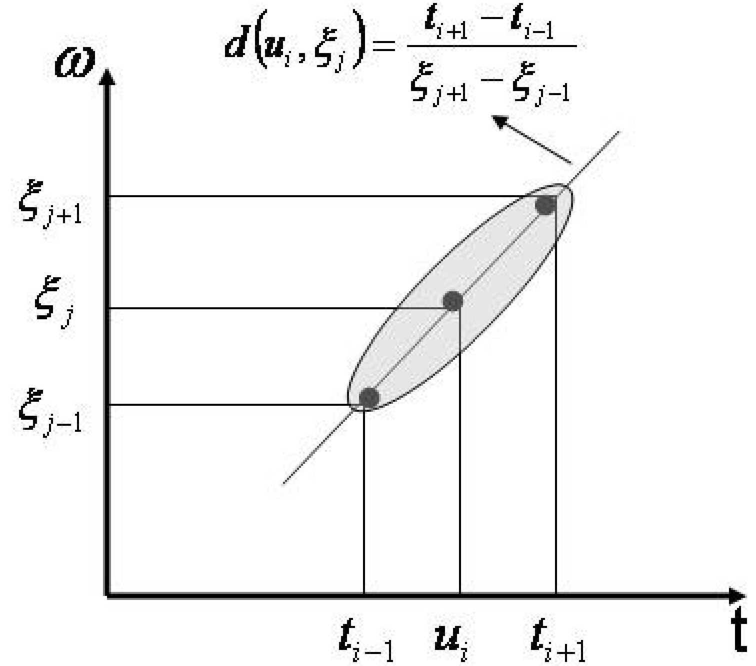

The time-frequency box in (u,ξ) can be obtained by rotating or shearing the time frequency box of standard STFT using the parameter d (u, ξ)

If d (u, ξ) is chosen based on the local wave dispersion, then the resulting time-frequency tiling will correspond to the entire wave dispersion behavior.

Time and Frequency Resolution

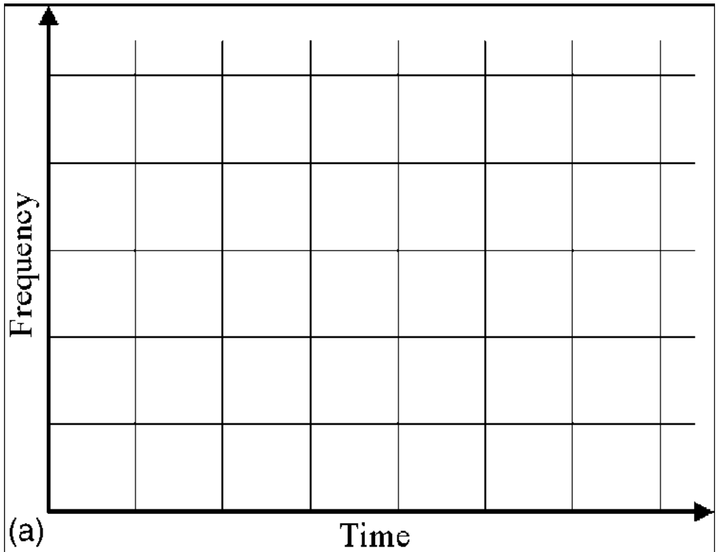

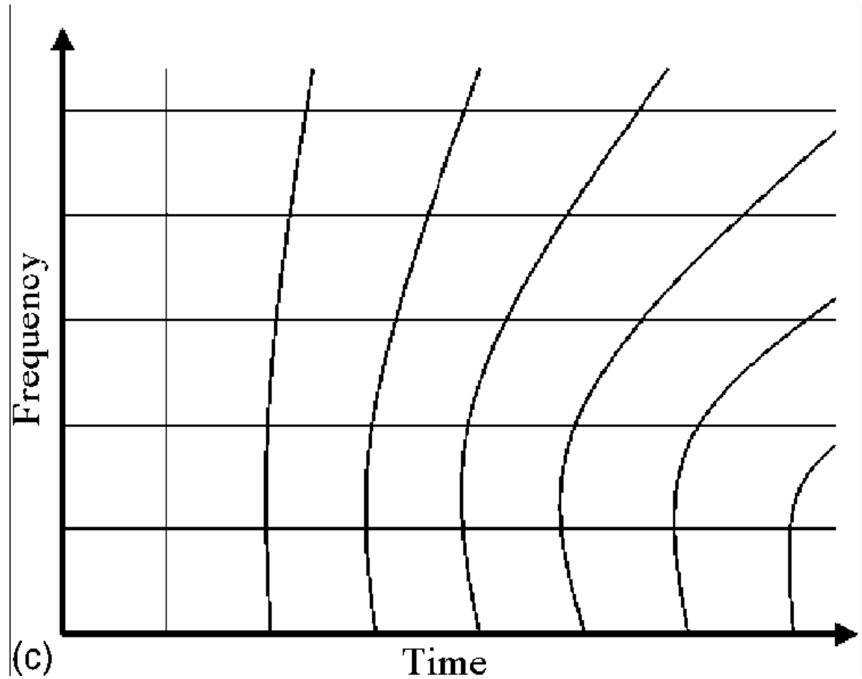

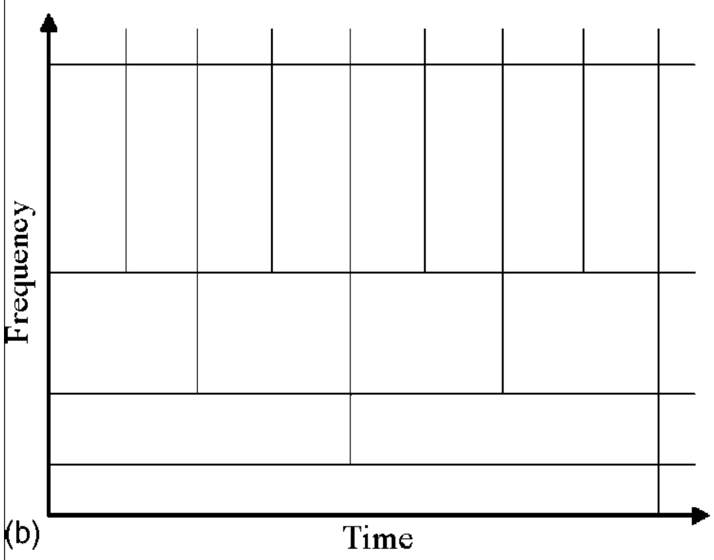

A comparison of time-frequency tilings.

b. Short-time Fourier transform

c. continuous wavelet transform

d. dispersion-based short-time Fourier transform.

Time – Frequency Diagrams

Modes 1, 2 and 3 are strong in the CSS signal

Modes 4, 5 and 6 partially present

Wavelet scalogram – poor time resolution at low frequencies

DSTFT performs well at the upper frequency band (compares well with wavelets)

At low frequencies DSTFT produces better time resolution.

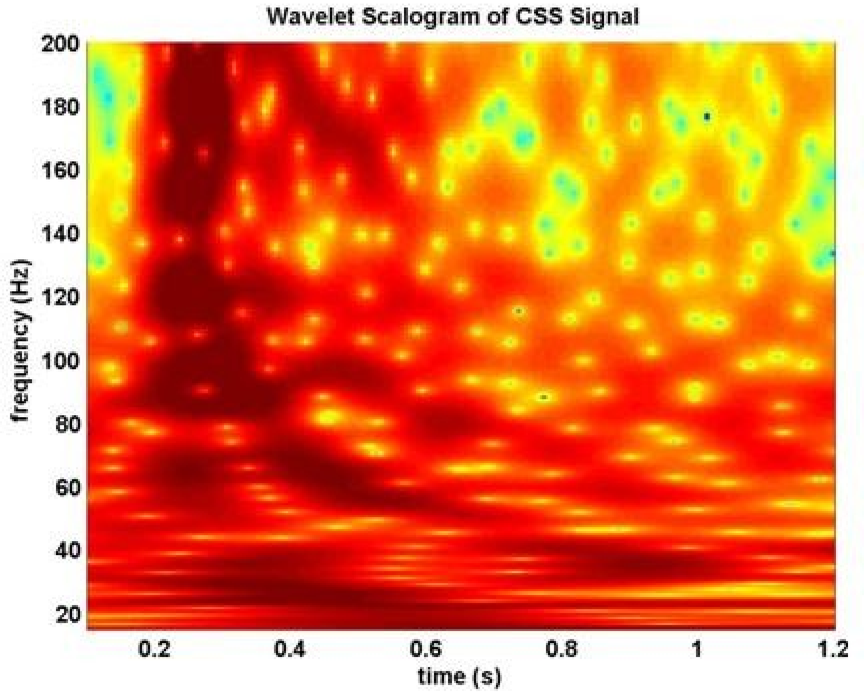

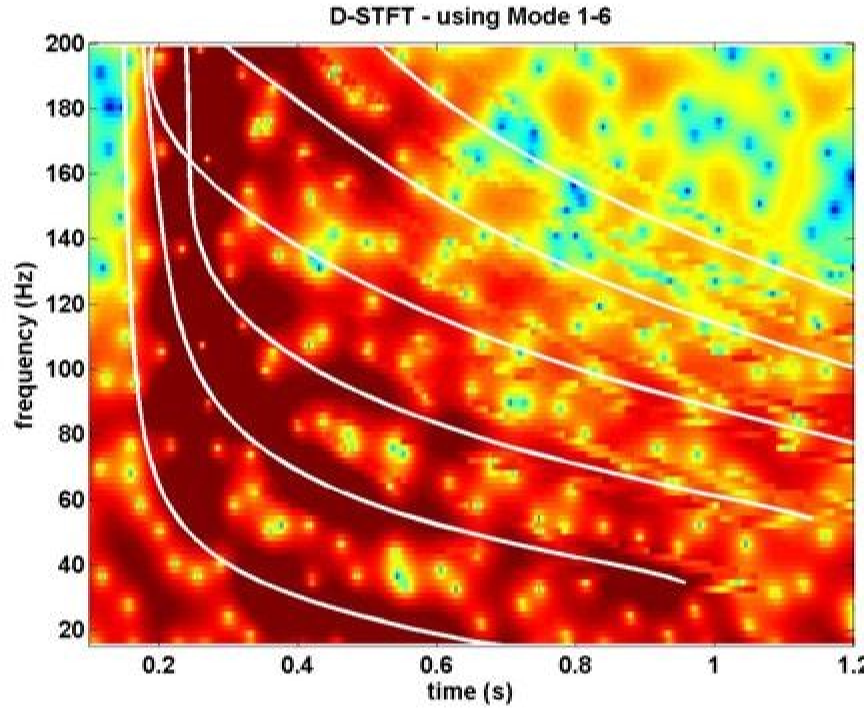

Iterative Scheme for estimating modal group speeds

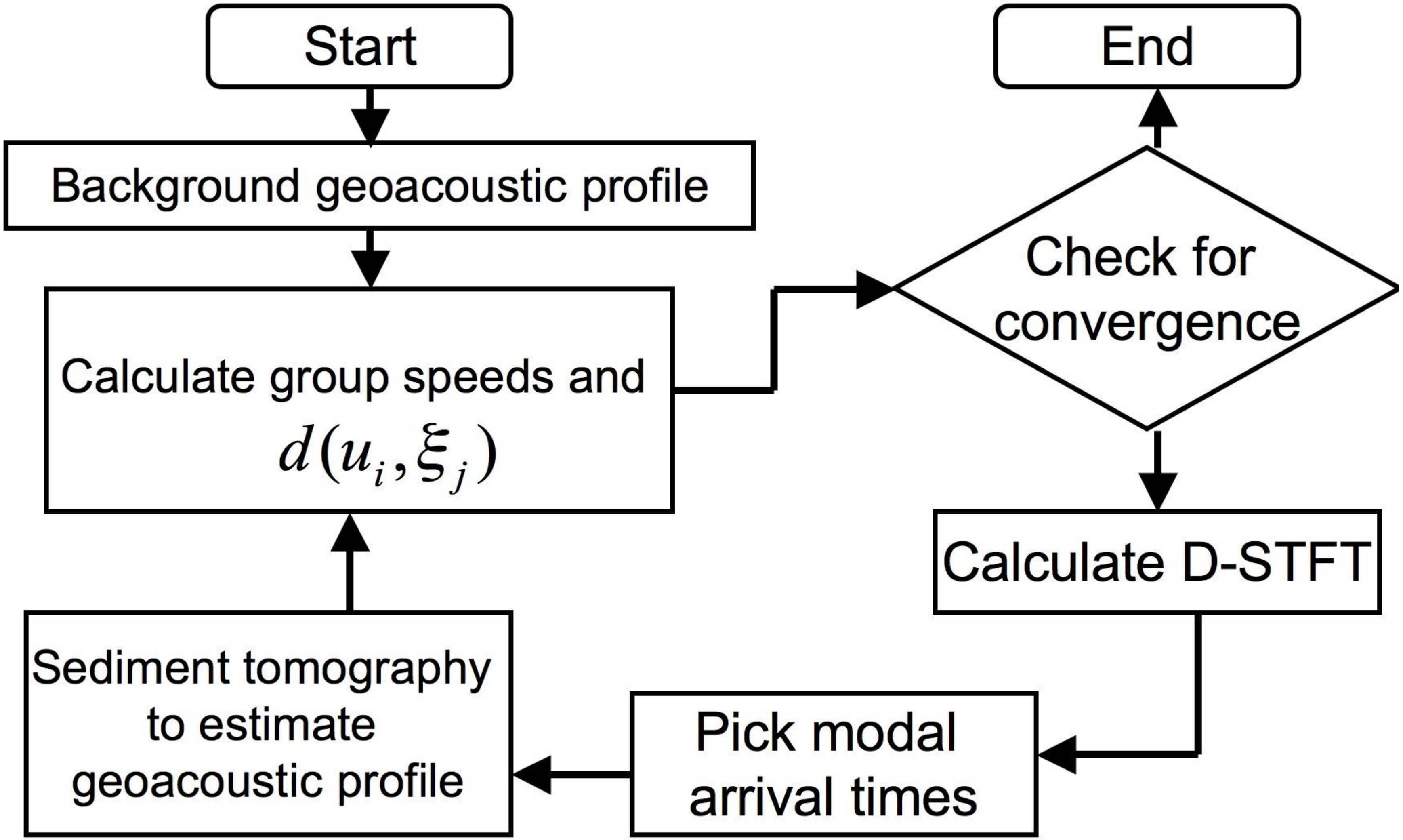

Inversion Results

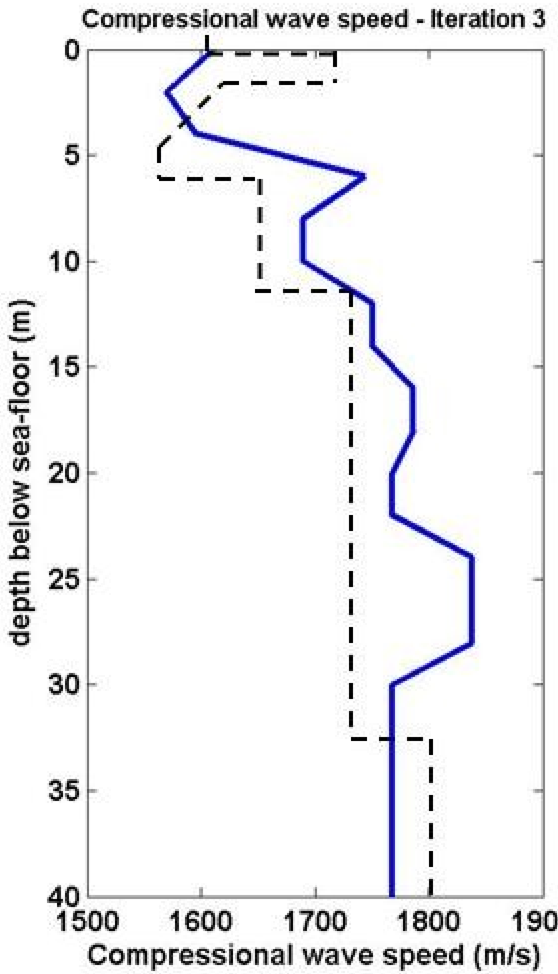

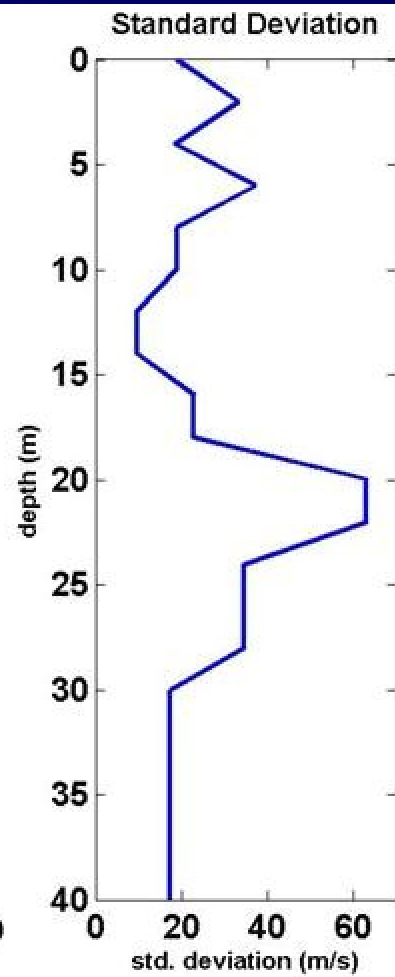

Compressional wave speed (top 40 m) compared with Jiang et al. model (JASA-2007)

Standard deviation ~ 20 m/sec.

The R- reflector is approx. around 20 m

Sea floor

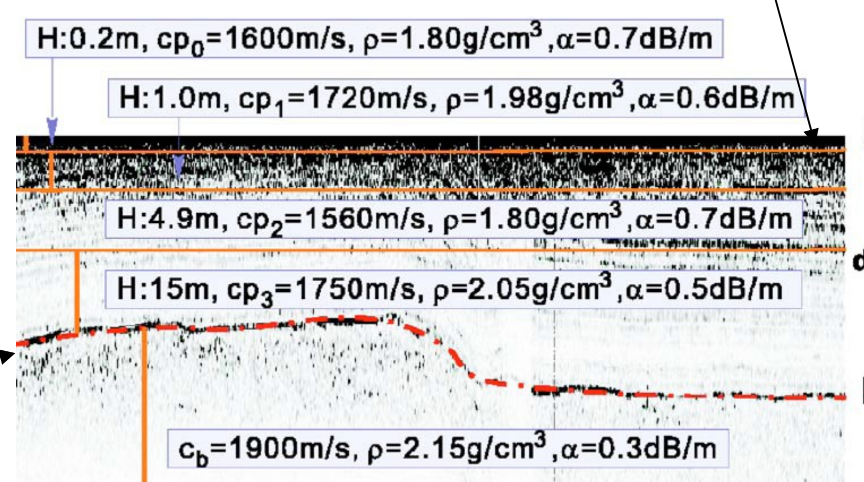

R - Reflector

Inversion Results

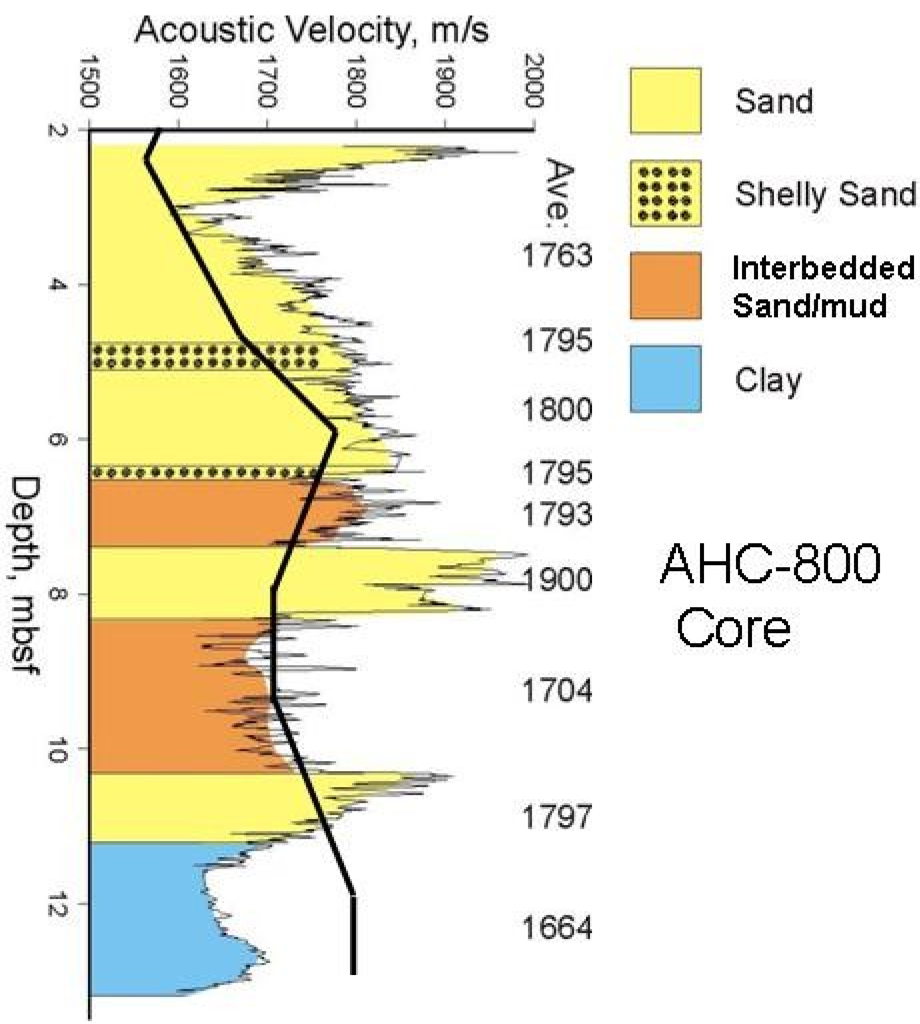

Sediments in top 15 m generally sandy interbedded with mud and shells.

Inversion captures the trend in core data; but lower in magnitude

Magnitude higher than Jiang et al. model.

Relative Sensitivity of modes

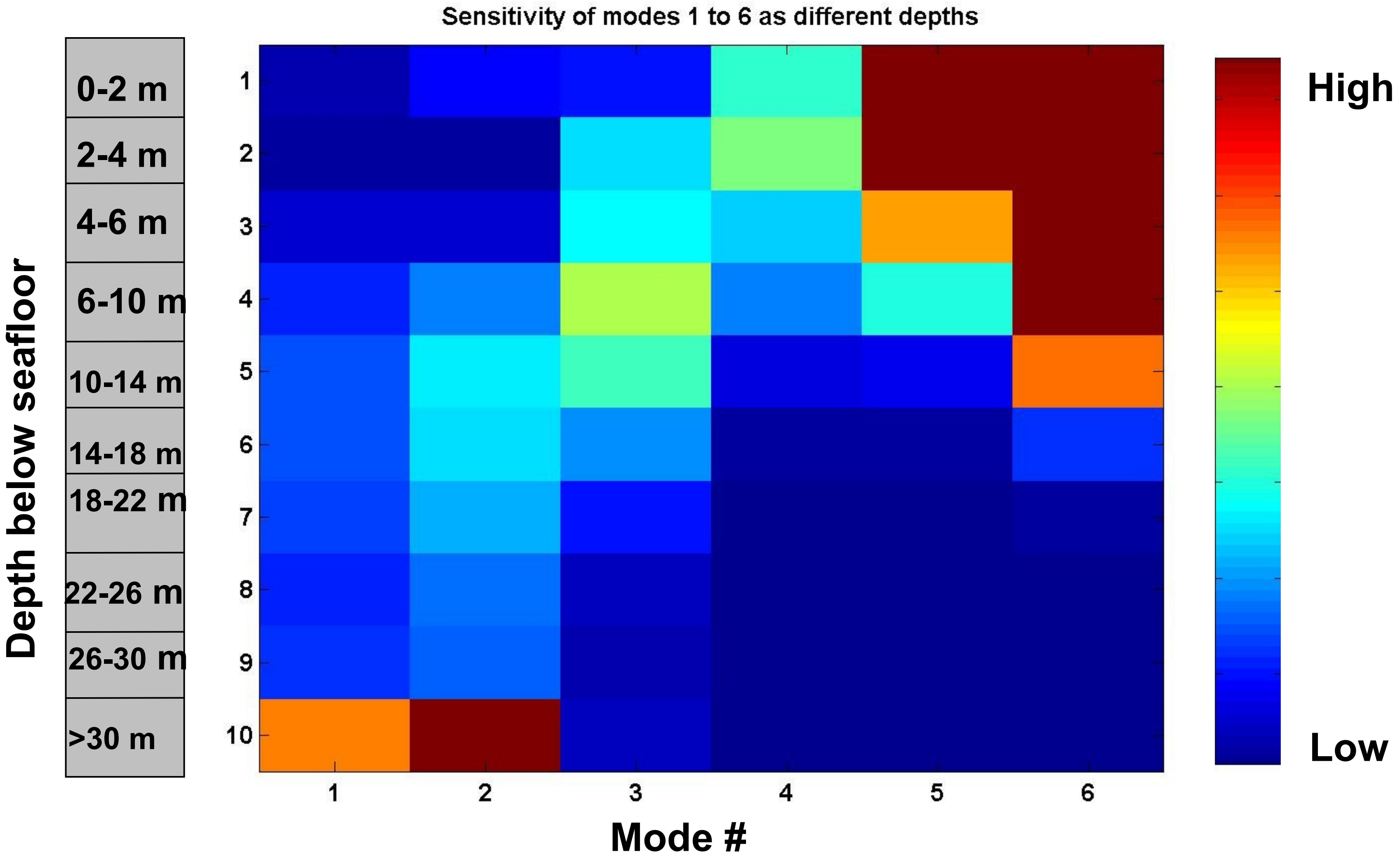

Attenuation Inversion

$$P_m(r,z) = \frac{i e^{-i\pi/4}}{\rho\sqrt{8\pi}\sqrt{r}}\,\psi(z_s)\,\psi(z)\,\frac{e^{i\kappa_m r}}{\sqrt{\kappa_m}}\,e^{-\beta_m r} \qquad \textbf{(1)}$$

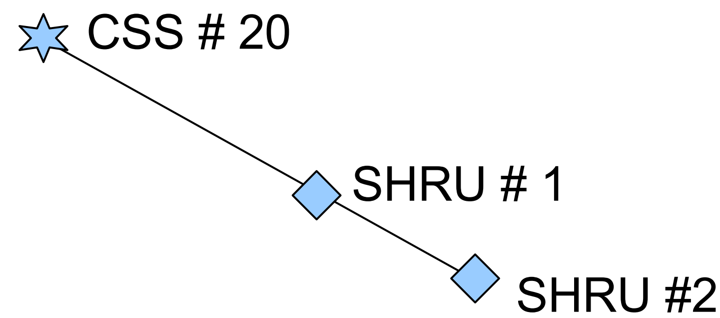

$$\frac{P_m(r1,z)}{P_m(r2,z)} = \sqrt{\frac{r1}{r2}}\,\frac{\psi_{m1}(z_{r1})}{\psi_{m2}(z_{r2})}\,\frac{e^{i\kappa_{m1} r1}}{e^{i\kappa_{m2} r2}}\,\frac{\sqrt{\kappa_{m1}}}{\sqrt{\kappa_{m2}}}\,\frac{e^{-\beta_m r1}}{e^{-\beta_m r2}} \qquad \textbf{(2)}$$

ρ	density	β	modal attenuation coefficient
r	source-receiver range	ψ	mode shape for mode m
z_{r1}, z_{r2}	receiver depths	$\alpha(z)$	attenuation profile
z	receiver depth	$k(z)$	$\omega / c(z)$
κ	horizontal propagation constant	ω	angular frequency

$$\kappa_m \beta_m = \int_0^\infty \alpha(z)\,k(z)\,|\psi_m(z)|^2\,dz$$

Inversion Algorithm

C(z) from CTD and Sediment inversions

k and n unknown parameters

α= k f^n

$$\kappa_{rm}\beta_m = \int_0^\infty \alpha(z)k(z)\left|\psi_m(z)\right|^2 dz$$

β – for different modes

Modal amplitude ratios (same mode and receiver depth, Different range)

$$\frac{P_m(r1,z)}{P_m(r2,z)} = \sqrt{\frac{r1}{r2}}\,\frac{\psi_{m1}(z_{s1})}{\psi_{m2}(z_{s2})}\,\frac{e^{i\kappa_{m1}r1}}{e^{i\kappa_{m2}r2}}\,\frac{\sqrt{\kappa_{m1}}}{\sqrt{\kappa_{m2}}}\,\frac{e^{-\beta_m r1}}{e^{-\beta_m r2}}$$

Minimize the difference between data and prediction

Mode amplitude ratios from Time-frequency diagrams

Best estimate k and n

Modal Amplitude Ratios

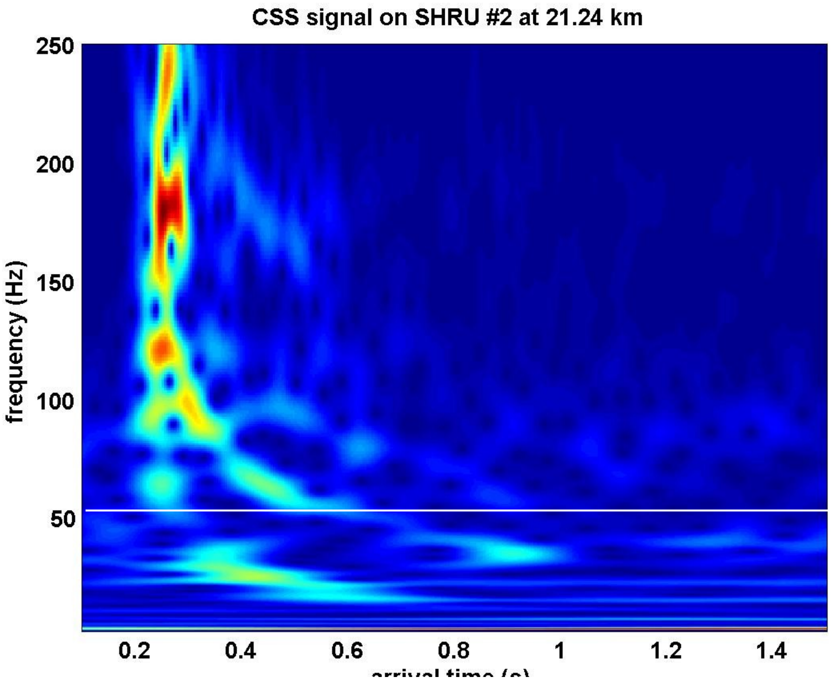

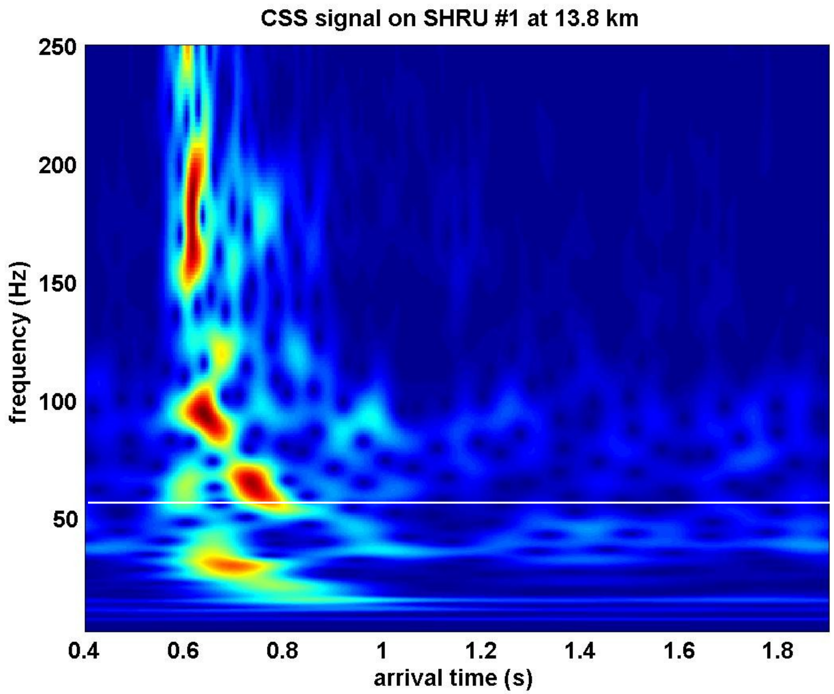

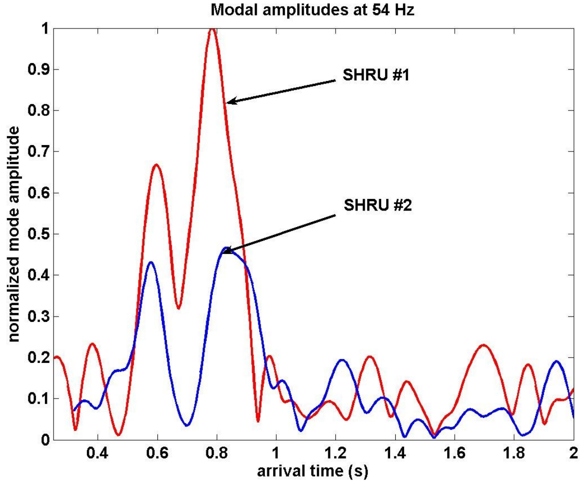

Mode 1 and 2 ratios in the frequency range 20 Hz to 80 Hz used for inversion

Inversion for attenuation in the sediment layer (0 to 18 m) and basement

Attenuation Inversion Results

Published data – all types of sediments (Stoll- 85)

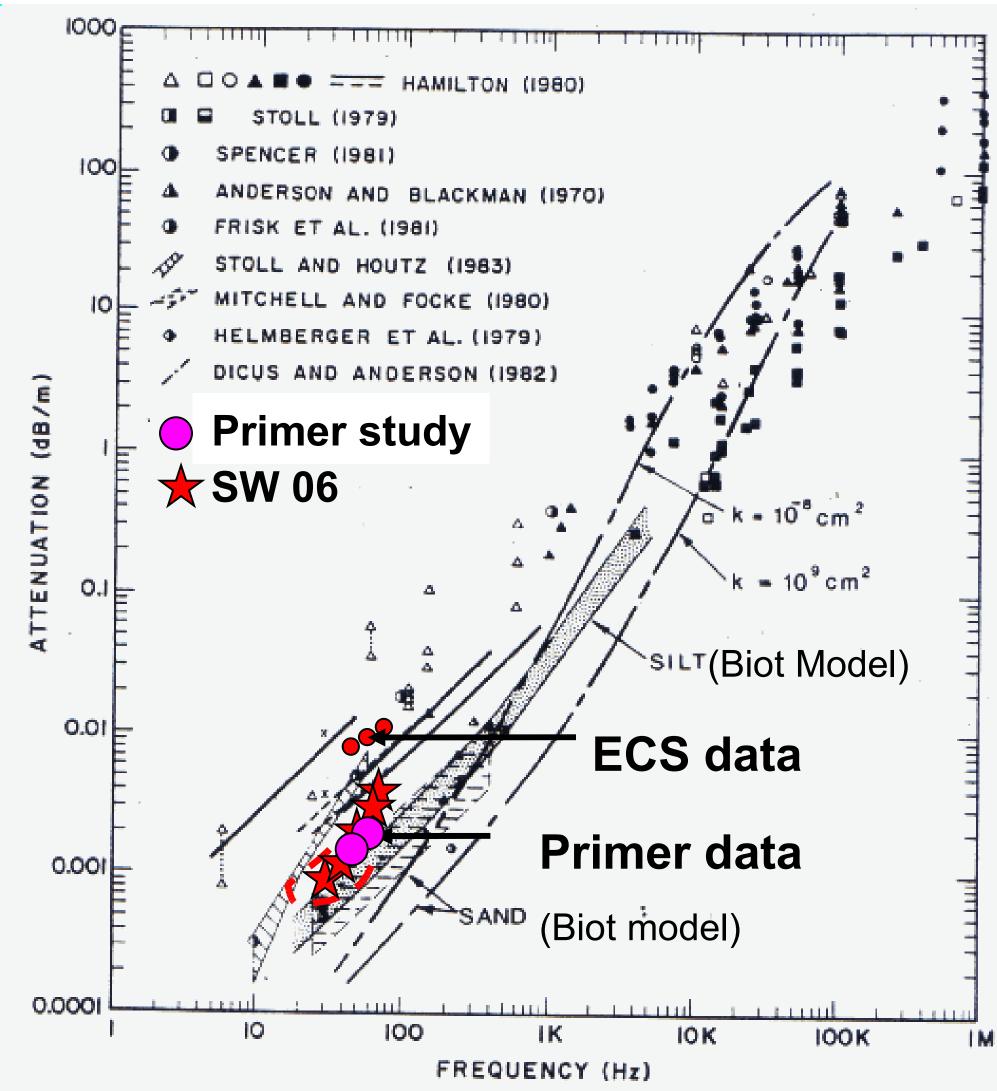

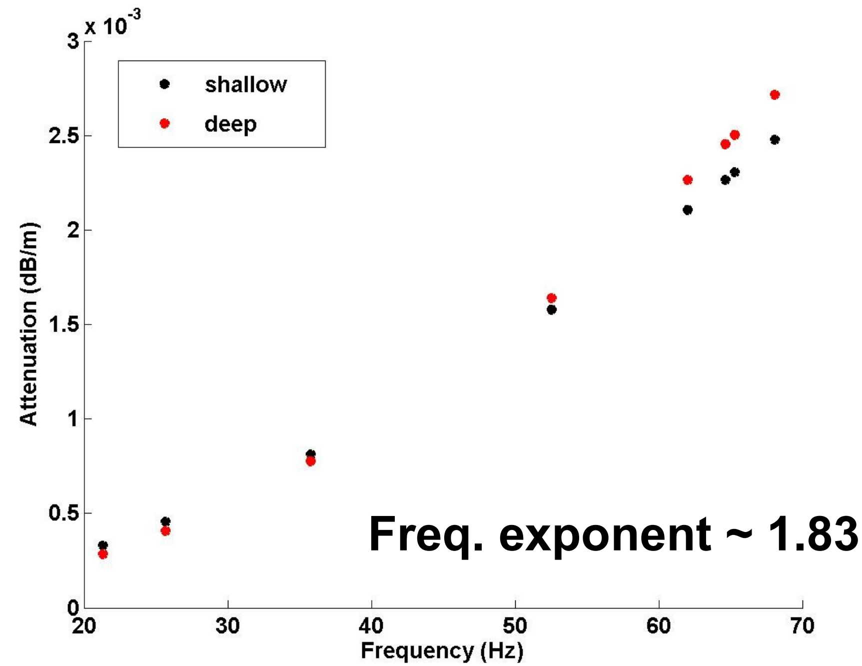

Inversions compare well with earlier (Primer) inversions

Frequency exponent agrees with Holmes et al. (JASA-EL;2007) value of 1.8 +/- 0.2

Summary and Future Work

- CSS provides a sharp impulse, and good low-frequency energy, and are environmentally friendly.
- D-STFT was applied to CSS data to improve the performance of time-frequency data.
- Initial inversions promising. Data from other CSSs and receivers could also be used.

Future Work

- Extensive inversions for attenuation
- Looking at the spatial variation using multiple sources and receivers

Questions ??

Schematic of CSS Deployment Used in SW06

1) generate gas/load chamber

2) deploy to depth and fire

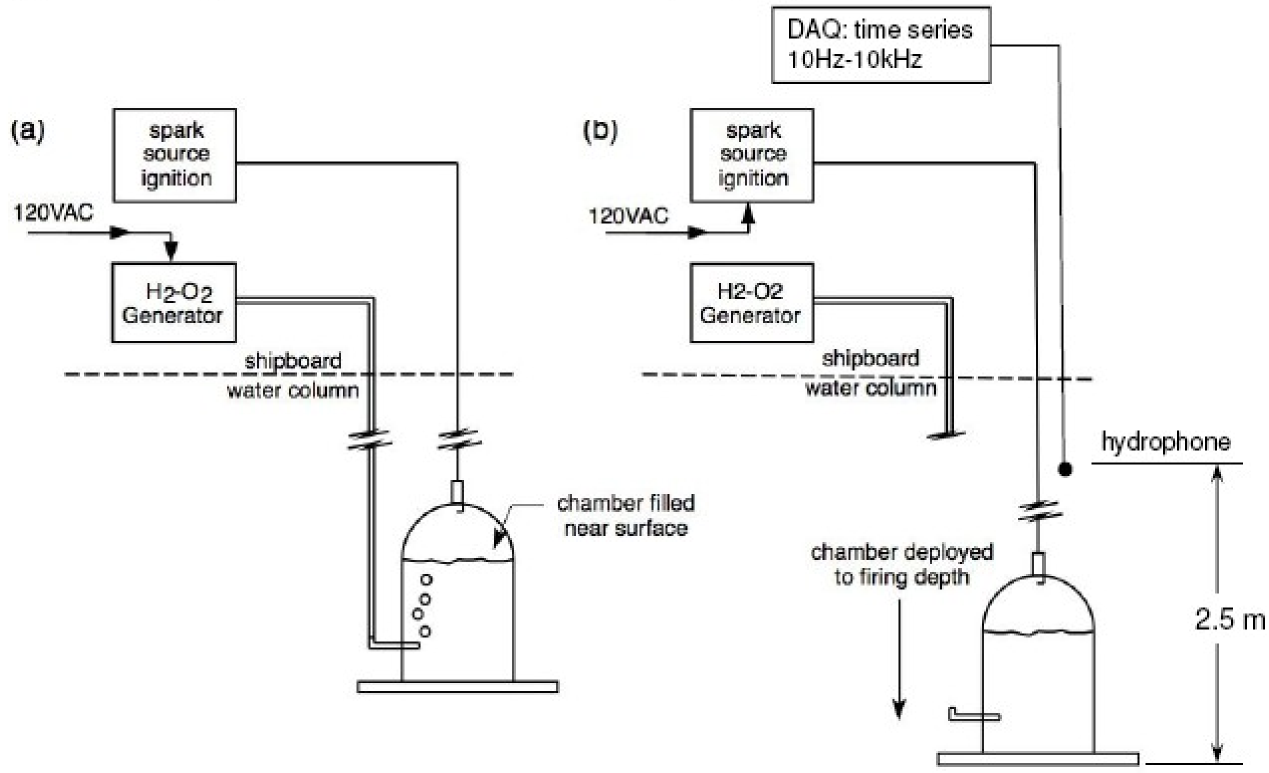

SW06 CSS System

Typical SW06 Pressure Signatures and Spectra

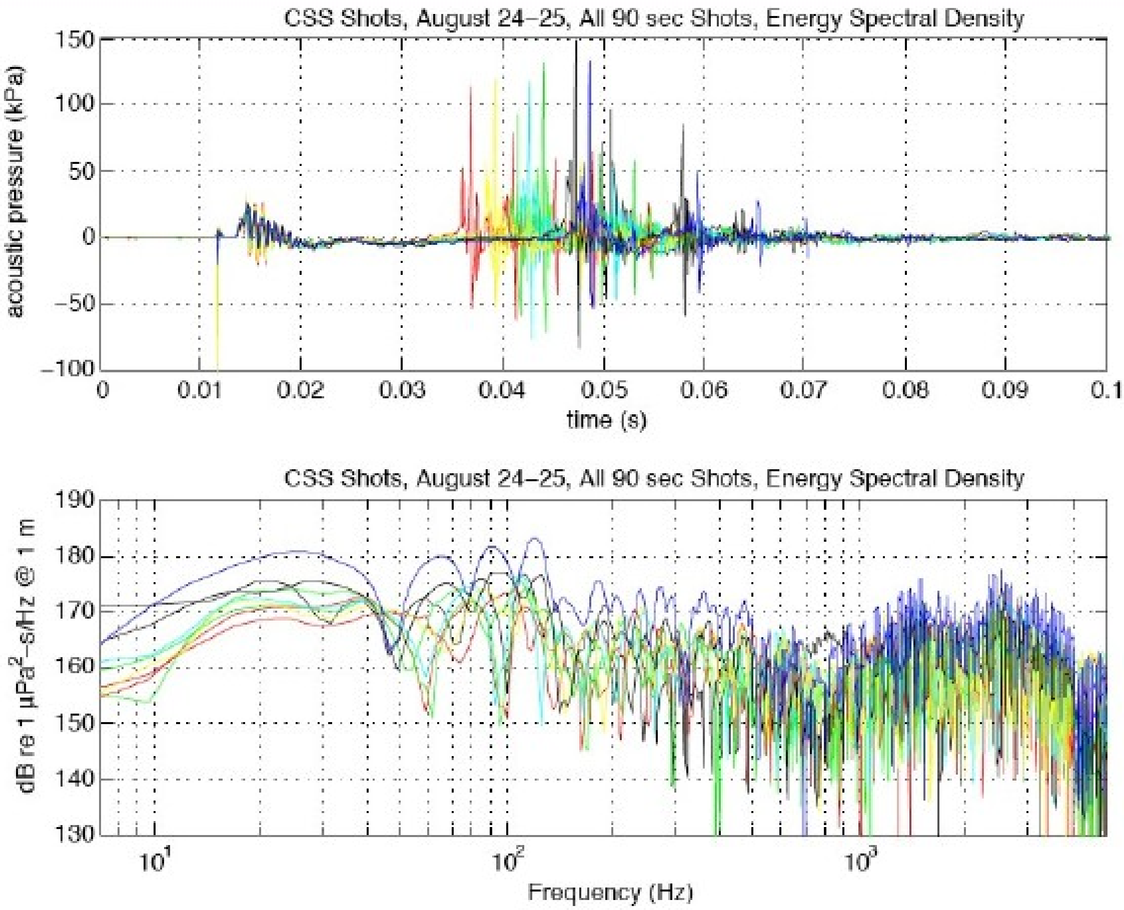

Comparison – D-STFT Vs Wavelet Scalogram

Modes 1, 2 and 3 D-STFT produces similar information
Mode 4 – possibly on a null
Mode 5 – D- STFT offers some promise as opposed to Scalogram

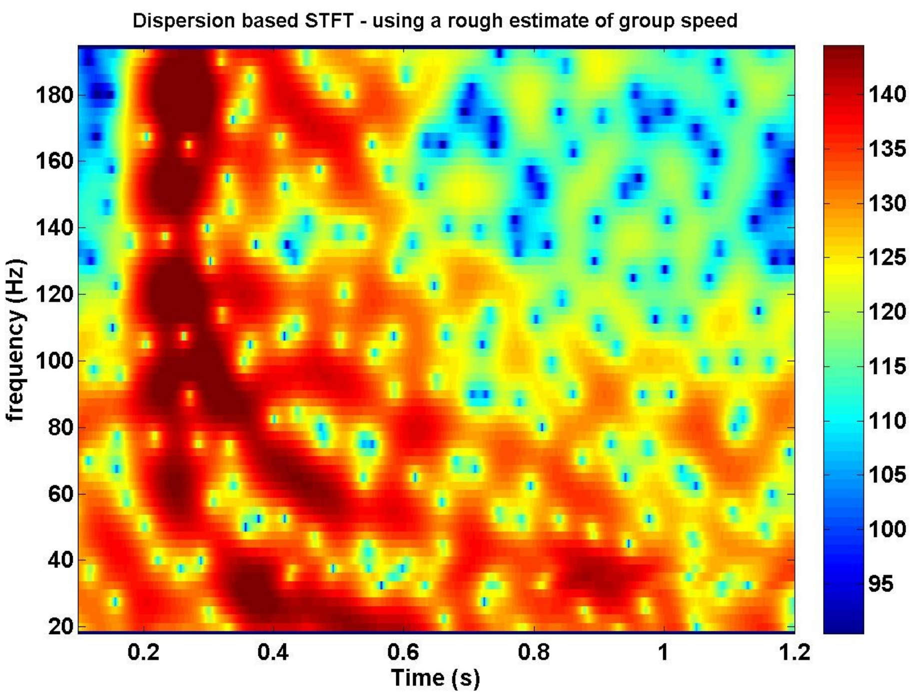

D-STFT

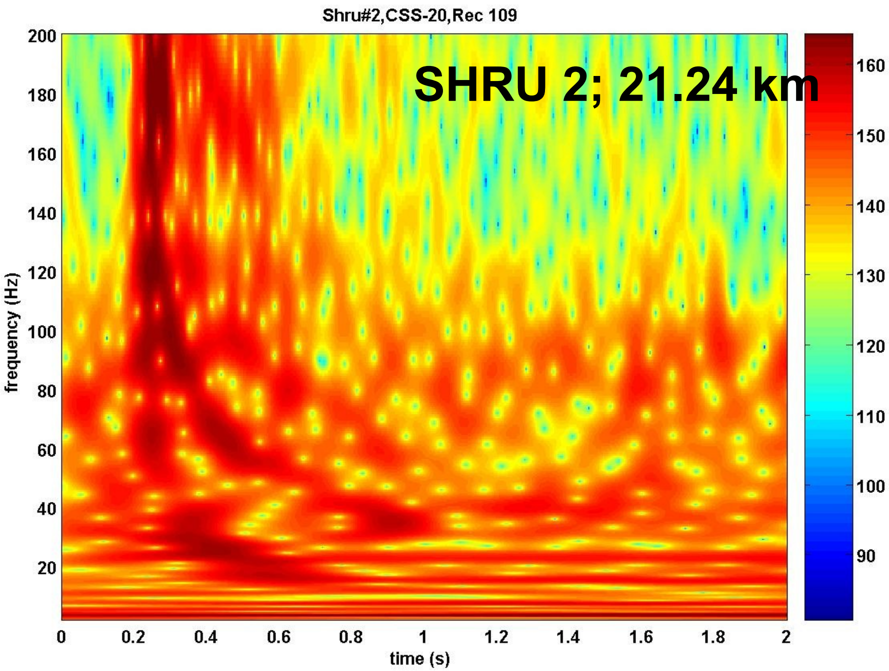

Wavelet Scalogram

Extra Slides – Locations of CSS events and SHRUs

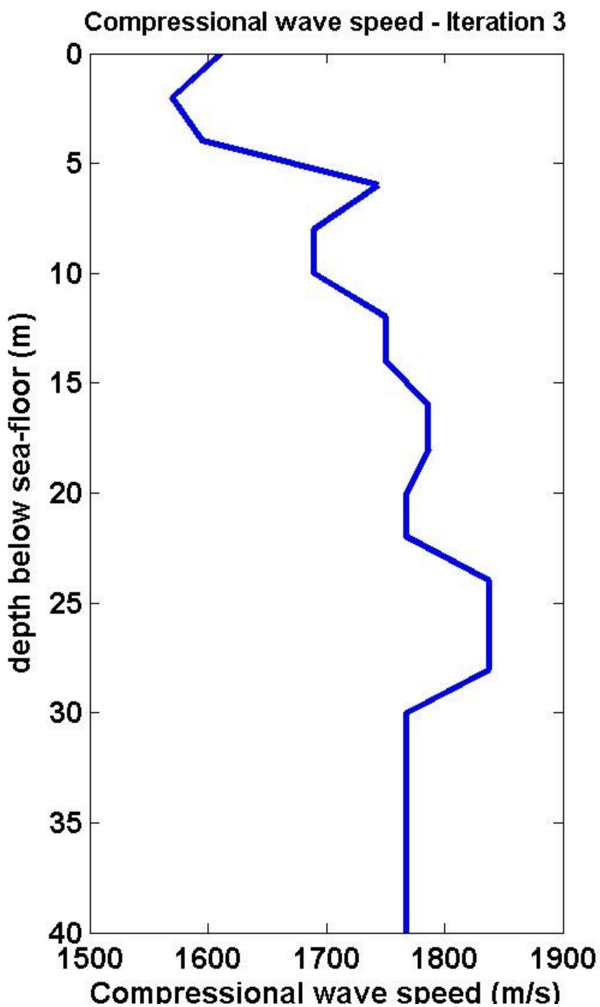
Compressional wave speed - Iteration 3
depth below sea-floor (m)
0
5
10
15
20
25
30
35
40
1500
1600
1700
1800
1900
Compressional wave speed (m/s)

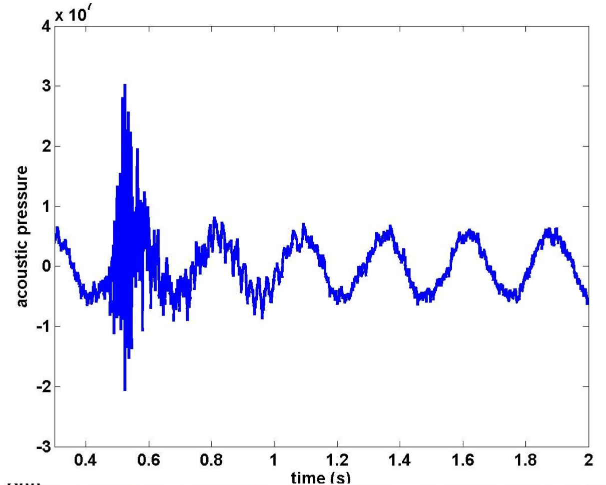
x 10^7
acoustic pressure
4
3
2
1
0
-1
-2
-3
0.4
0.6
0.8
1
1.2
1.4
1.6
1.8
2
time (s)

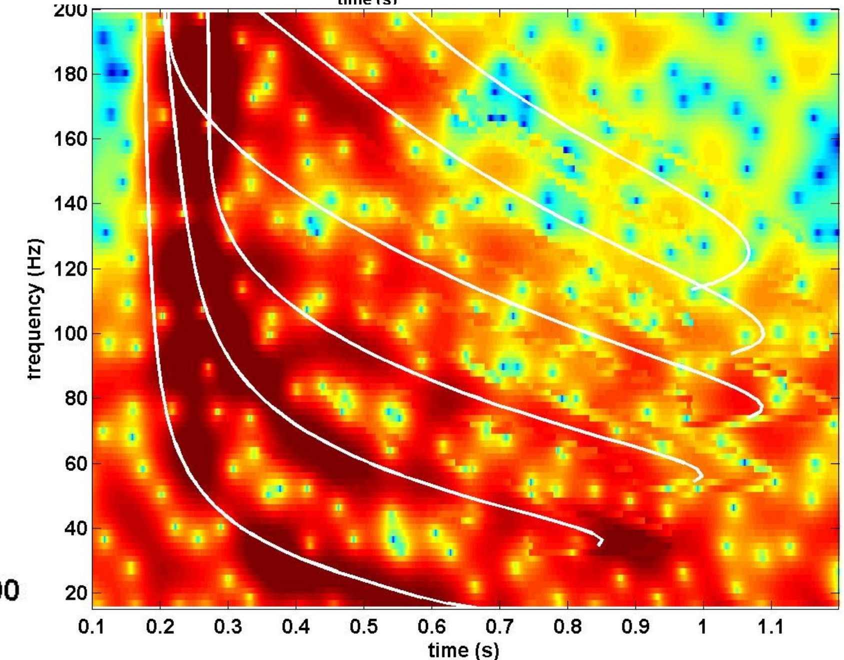
frequency (Hz)
200
180
160
140
120
100
80
60
40
20
0.1
0.2
0.3
0.4
0.5
0.6
0.7
0.8
0.9
1
1.1
time (s)

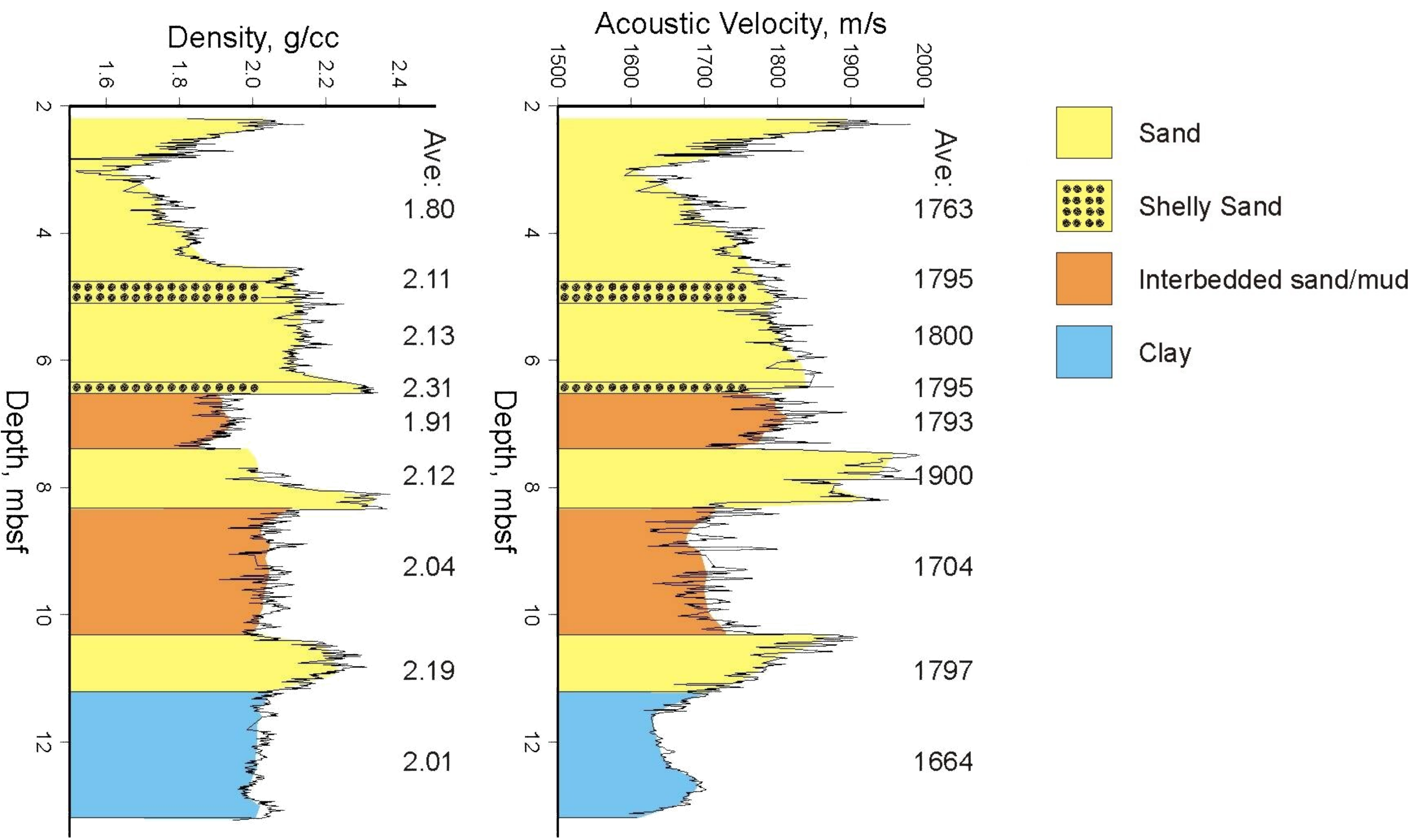
Density, g/cc
1.6
1.8
2.0
2.2
2.4
Depth, mbsf
Ave:
1.80
2.11
2.13
2.31
1.91
2.12
2.04
2.19
2.01
Acoustic Velocity, m/s
1500
1600
1700
1800
1900
2000
Depth, mbsf
Ave:
1763
1795
1800
1795
1793
1900
1704
1797
1664
Sand
Shelly Sand
Interbedded sand/mud
Clay

AHC-800 Core

Short core at station 77

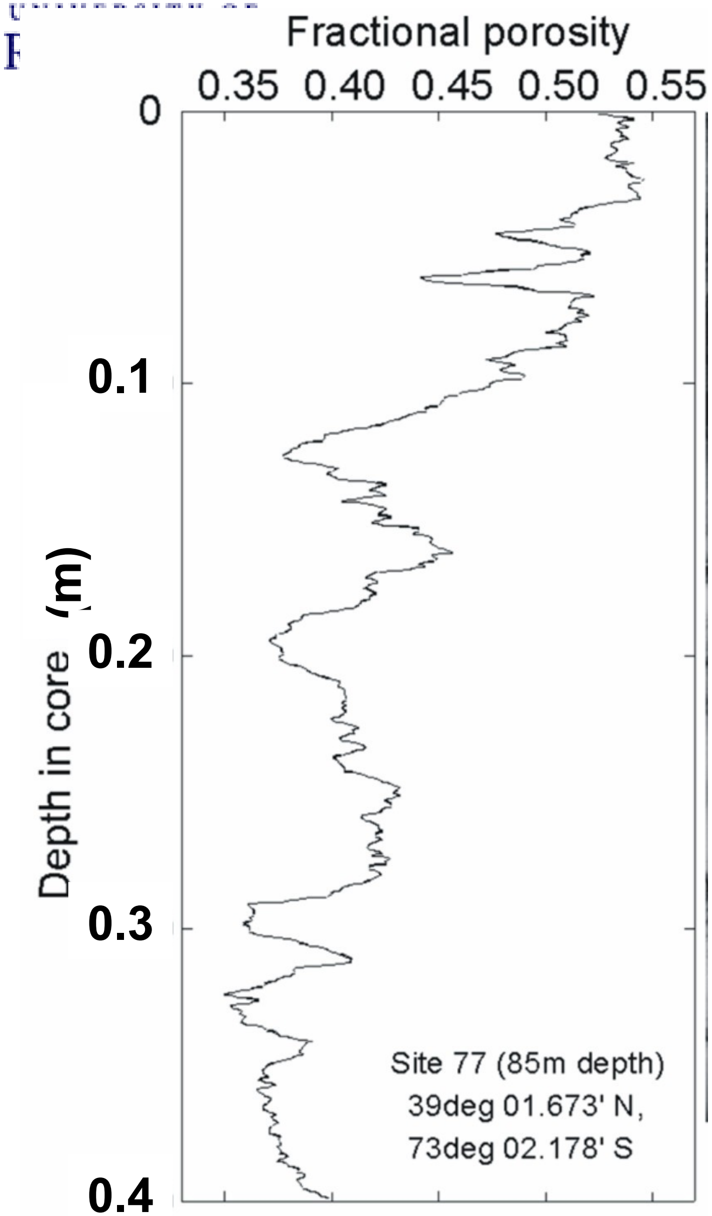

From Chris Sommerfield

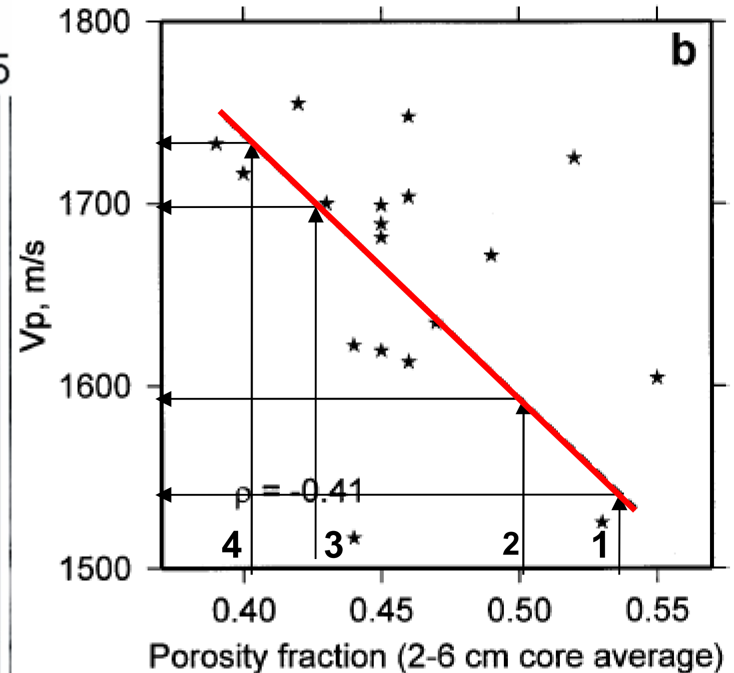

No.	Latitude(N)	Longitude(W)	Velocity(m/s)
1	39.03689	-73.05421	1726.0
2	39.03556	-73.05193	1729.0
3	39.02733	-73.03603	1733.0
4	39.01654	-73.04579	1721.0
5	38.99951	-73.07311	1743.0

In situ probe data

Inversion : YT

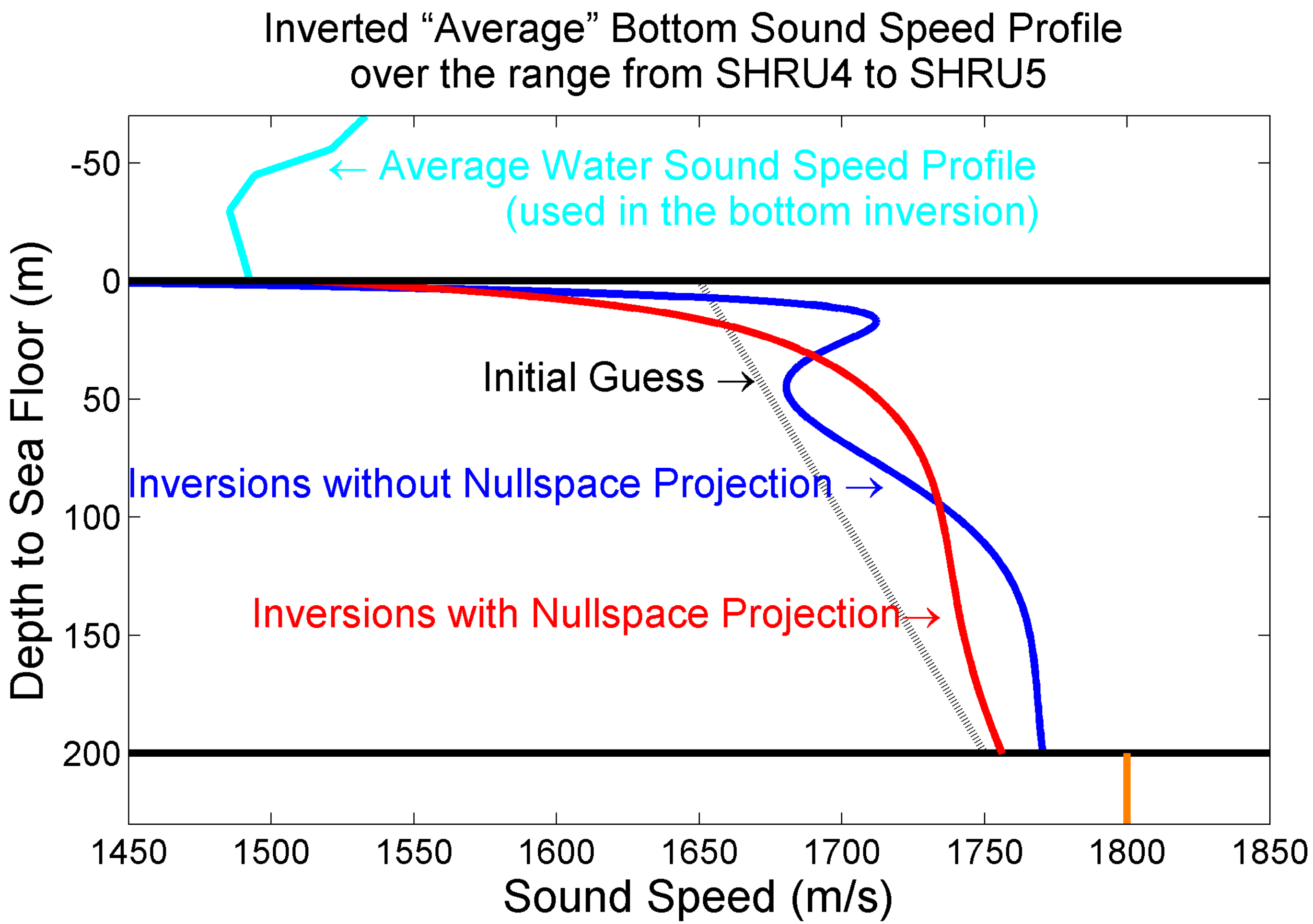

Dip Line – Preliminary Interpretation

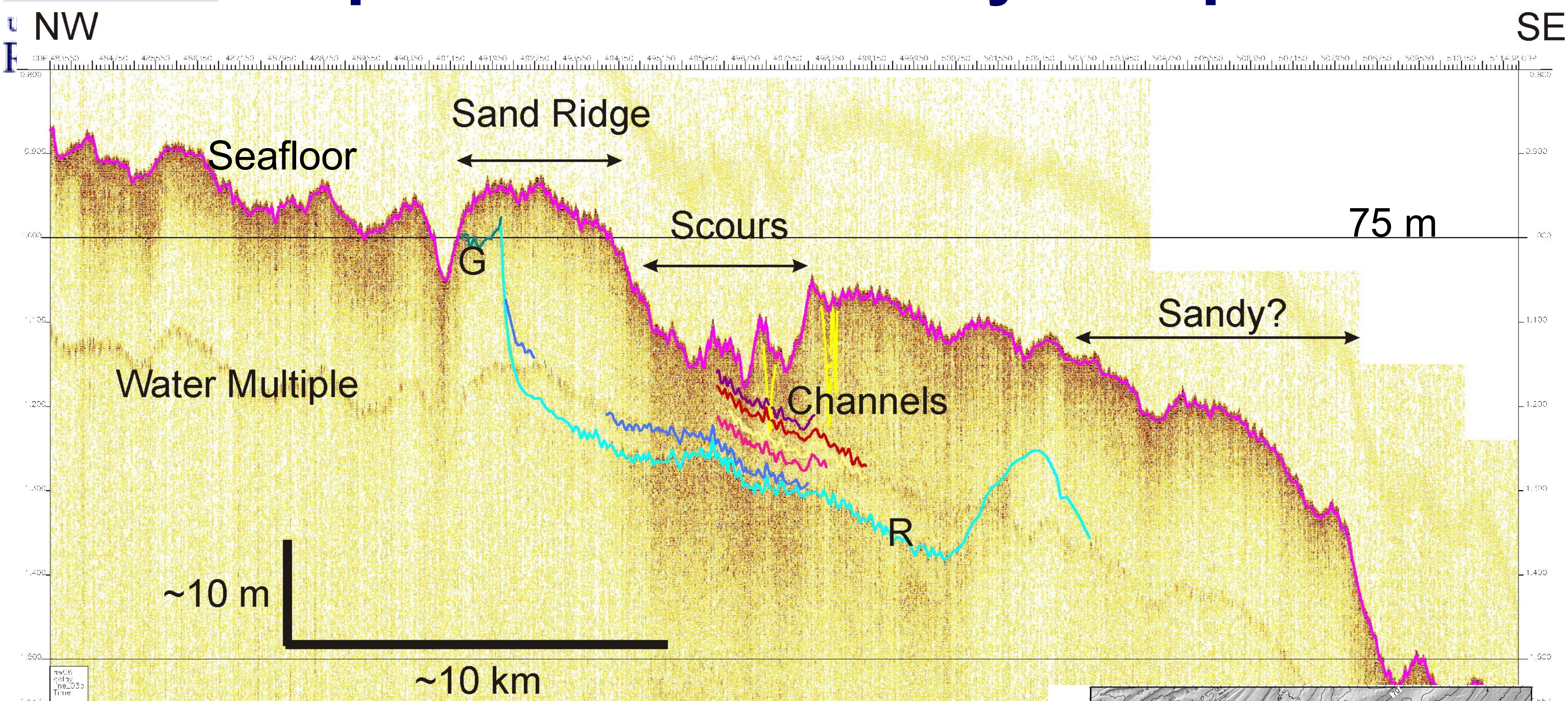

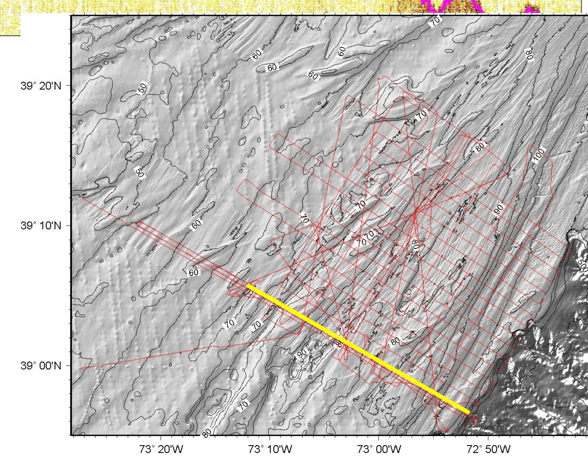

Toward the southern end of the survey area, the outer shelf becomes increasingly **less** acoustically penetrative – probably indicative of higher sand/gravel content at the surface.

From: John Goff